

## Bisintercalating Threading Diacridines: Relationships between DNA Binding, Cytotoxicity, and Cell Cycle Arrest

Laurence P. G. Wakelin,<sup>\*,†</sup> Xianyong Bu,<sup>†</sup> Alexandra Eleftheriou,<sup>†</sup> Alpesh Parmar,<sup>†</sup> Charbel Hayek,<sup>†</sup> and Bernard W. Stewart<sup>‡,§</sup>

School of Medical Sciences, and the School of Women's and Children's Health, University of New South Wales, Sydney 2052, New South Wales, Australia, and Public Health Unit, South East Sydney Area Health Service, Sydney 2031, New South Wales, Australia

Received May 27, 2003

We have synthesized a series of bis(9-aminoacridine-4-carboxamides) linked via the 9-position with neutral flexible alkyl chains, charged flexible polyamine chains, and a semirigid charged piperazine-containing chain. The carboxamide side chains comprise *N,N*-dimethylaminoethyl and ethylmorpholino groups. The compounds are designed to bisintercalate into DNA by a threading mode, in which the side chains are intended to form hydrogen-bonding contacts with the O6/N7 atoms of guanine in the major groove, and the linkers are intended to lie in the minor groove. By this means, we anticipate that they will dissociate slowly from DNA, and be cytotoxic as a consequence of template inhibition of transcription. The dimers remove and reverse the supercoiling of closed circular DNA with helix unwinding angles ranging from 26° to 46°, confirming bifunctional intercalation in all cases, and the DNA complexes of representative members dissociate many orders of magnitude more slowly than simple aminoacridines. Cytotoxicity for human leukemic CCRF–CEM cells was determined, the most active agents having IC<sub>50</sub> values of 35–50 nM in a range extending over 20-fold, with neither the dimethylaminoethyl nor the ethylmorpholino series being intrinsically more toxic. In common with established transcription inhibitors, the morpholino series, with one exception, have no effect on cell cycle distribution in randomly dividing CCRF–CEM populations. By contrast, the dimethylaminoethyl series, with two exceptions, cause G2/M arrest in the manner of topoisomerase poisons, consistent with possible involvement of topoisomerases in their mode of action. Thus, the cellular response to these bisintercalating threading agents is complex and appears to be determined by both their side chain and linker structures. There are no simple relationships between structure, cytotoxicity, and cell cycle arrest, and the origins of this complexity are unclear given that the compounds bind to DNA by a common mechanism.

### Introduction

DNA-intercalating agents inhibit cell growth by two well-established mechanisms: poisoning topoisomerases<sup>1–3</sup> and inhibiting transcription.<sup>4</sup> Clinically useful topoisomerase poisons include the anthracyclines doxorubicin and daunomycin, the anthracenedione mitoxantrone, and the 9-anilinoacridine amsacrine.<sup>1–3</sup> Trapping of transient topoisomerase–DNA cleavable complexes by these drugs leads to clastogenesis, cell cycle arrest, and apoptosis.<sup>1–3</sup> Related experimental cytotoxins based on acridine-4-carboxamide chromophores, such as *N*-[2-(dimethylamino)ethyl]acridine-4-carboxamide, known as DACA, as well as its 9-amino derivatives, also trap topoisomerase cleavable complexes,<sup>5,6</sup> and DACA is in phase II clinical trials.<sup>7</sup> Intercalating transcription inhibitors are exemplified by the antitumor antibiotics actinomycin D, echinomycin, and nogalamycin.<sup>8–10</sup> Actinomycin D is a monofunctional intercalator,<sup>8</sup> echinomycin is a bisintercalating agent,<sup>9</sup> and nogalamycin is a monofunctional intercalator bearing two sugar sub-

stituents that binds by a threading mode.<sup>10</sup> In the nogalamycin–DNA complex, one sugar ring lies in the DNA minor groove and the other makes hydrogen-bonding interactions with the O6/N7 atoms of guanine in the major groove. Actinomycin D is used in the treatment of Wilm's tumor and childhood sarcomas, and echinomycin has been widely assessed in phase II clinical trials.<sup>11,12</sup>

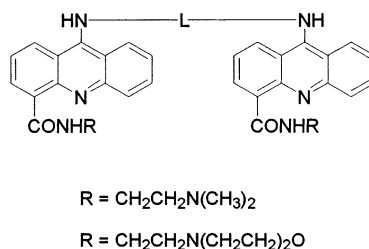
A characteristic shared by the transcription inhibitors discussed is that they bind to DNA reversibly with modest affinities in the range 10<sup>5</sup>–10<sup>7</sup> M<sup>-1</sup>, placing bulky groups in the minor groove covering four to six basepairs, and form long-lived complexes that impede the progression of RNA polymerases.<sup>8–10,13–16</sup> This ability to form slowly dissociating DNA complexes, with half-lives of hundreds of seconds, distinguishes the transcription inhibitors from the topoisomerase poisons, which dissociate from DNA rapidly in the millisecond to second time range.<sup>17–19</sup> While intercalating topoisomerase poisons have been widely investigated as potential antitumor agents,<sup>1–3</sup> scant attention has been paid to the similar development of template transcription inhibitors, despite their impressive experimental antitumor activity (see citations in refs 4, 8–10, and 13–16). This is, in part, because of the difficulty of endowing chemically accessible compounds with the capacity to

\* To whom correspondence should be addressed. Phone: +61-2-9385 2563. Fax: +61-2-9385 1059. E-mail: l.wakelin@unsw.edu.au.

<sup>†</sup> School of Medical Sciences, University of New South Wales.

<sup>‡</sup> School of Women's and Children's Health, University of New South Wales.

<sup>§</sup> Public Health Unit, South East Sydney Area Health Service.



Linker	Linker name	Flexibility	Linker charge	Interchromophore distance, Å <sup>1</sup>
(CH <sub>2</sub> ) <sub>6</sub>	C6	Flexible	Neutral	8.8
(CH <sub>2</sub> ) <sub>8</sub>	C8	Flexible	Neutral	11.3
(CH <sub>2</sub> ) <sub>3</sub> NH(CH <sub>2</sub> ) <sub>3</sub>	C3NC3	Flexible	+1	9.8
(CH <sub>2</sub> ) <sub>3</sub> NH(CH <sub>2</sub> ) <sub>4</sub>	C3NC4	Flexible	+1	11.4
(CH <sub>2</sub> ) <sub>2</sub> NH(CH <sub>2</sub> ) <sub>2</sub> NH(CH <sub>2</sub> ) <sub>2</sub>	C6N2	Flexible	+2	11.3
(CH <sub>2</sub> ) <sub>2</sub> N(CH <sub>2</sub> CH <sub>2</sub> ) <sub>2</sub> N(CH <sub>2</sub> ) <sub>2</sub>	C2pipC2	Semi-rigid	+2	10.1

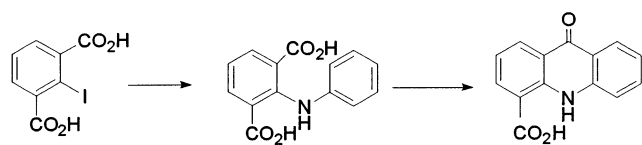
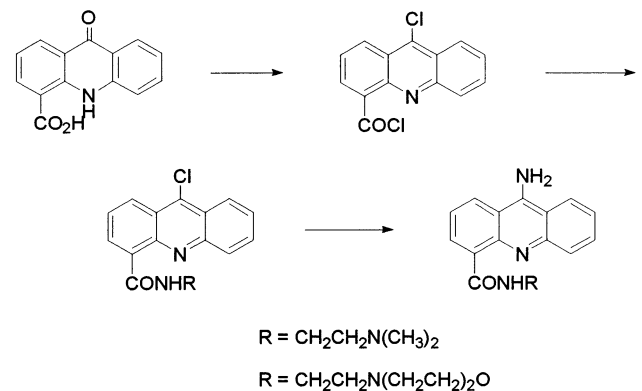
**Figure 1.** Structure of the threading diacridines studied.  $-\text{N}(\text{CH}_2\text{CH}_2)_2\text{N}-$  denotes piperazine. <sup>1</sup>Data taken from ref 27.

form long-lived reversible complexes that occupy approximately half a turn of the helix in the minor groove, down which RNA polymerases track. Here, we describe our initial attempts to develop agents intended to meet these requirements and to be cytotoxic as a consequence of inhibiting transcription.

Our approach exploits a structural motif that combines the bisintercalation of echinomycin with the threading mode of nogalamycin. The novel agents are dimers of 9-aminoacridine-4-carboxamide joined via the 9-amino group by various linkers, and bear one of two different 4-carboxamide threading side chain "hooks" (Figure 1). Recently, by crystallographic analysis, we have established that nonthreading versions of the 9-aminoacridine-4-carboxamides with the same side chains as used here, *N,N*-dimethylaminoethyl and ethylmorpholino groups, bind to DNA with the side chains lying in the major groove, forming hydrogen-bonding interactions with the O6 and N7 atoms of guanine in a manner similar to the amino sugar of nogalamycin.<sup>21,22</sup> Thus, we anticipate that the bisthreading agents will bind with their carboxamide side chains making analogous bonding contacts with guanines in the major groove, and that their linkers, comprising neutral flexible alkyl chains, charged flexible polyamine chains, and a semirigid charged piperazine-containing chain, will come to lie in the minor groove. By binding in this manner, the side chains are intended to behave as "barbed spears" that do not excessively hinder intercalation as they thread through the helix but that make withdrawal of the intercalated chromophores difficult as a consequence of their guanine interactions. In previous work with monofunctional threading agents of this kind, based on 9-anilinoacridine-4-carboxamides, we have demonstrated a substantial increase in complex lifetime, without enhancing affinity, as a result of this binding mode.<sup>20</sup> This uncoupling of thermodynamics and kinetics is a consequence of the slower rate of intercalation associated with the requirement to thread the side chain through the DNA duplex<sup>20</sup>. The ability to dissociate slowly, yet bind with modest affinity, is an important element in the design of the threading dimers, since

solid tumor activity of intercalating agents is limited by their capacity to penetrate into tumor masses, and this is in part determined by their DNA affinity.<sup>23</sup> This feature distinguishes our work from that of Chaires and colleagues, who have sought to enhance the activity of the anthracycline topoisomerase II poisons by developing nonthreading dimers with exceptionally high DNA-binding constants.<sup>24</sup> In collaboration with Iverson and others, Chaires has also described a series of highly cationic, peptide-linked, polyintercalating agents based on naphthalenetetracarboxylic diimides, which appear to thread their interchromophore linkers through the DNA helix.<sup>25</sup> These agents are active against bacteria but are not toxic to mammalian cell lines,<sup>26</sup> presumably because of transport and/or metabolic stability problems. Given that the bisthreading compounds described here are designed to dissociate slowly from DNA, with the purpose of inhibiting transcription, and yet are composed of elements known to poison topoisomerases, we further anticipate that their biological properties might reflect this dual character. Such dual activity, should it occur, may prove beneficial in circumventing the development of drug resistance selected by "single character" agents.

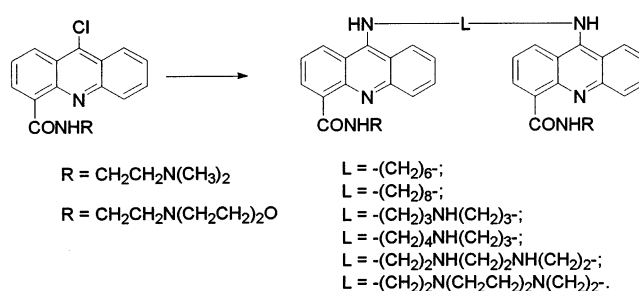
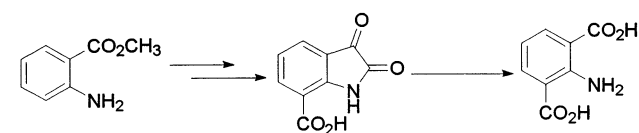
We have sought to determine the extent to which the interaction of the bis(9-aminoacridine-4-carboxamides) with DNA is anticipated by molecular modeling, and whether relative cytotoxic activity, as well as the mode of cell killing, can be related to variations in linker and side chain structure. To establish their capacity to bisintercalate, we measured their helix unwinding angles as determined by the ability to remove and reverse the supercoiling of covalently closed circular DNA.<sup>27</sup> Poisoning of topoisomerase II activity is almost invariably accompanied by cell cycle arrest at the G2/M boundary<sup>28,29</sup> and is often followed by cell death: a desirable scenario so far as the response of malignant cells to putative cytotoxic drugs is concerned.<sup>30,31</sup> In the present work, we assessed cell cycle distribution by flow cytometry after treatment of the human lymphoblastoid T-cell line CCRF-CEM. Such analysis also provides an indication of cell death, by dint of the accumulation of

**Scheme 1.** Synthesis of Acridone-4-carboxylic acid**Scheme 2.** Synthesis of 9-Aminoacrididine-4-carboxamides

cells having less than G1 DNA content.<sup>32</sup> For the purposes of providing comparative data with type-specific examples of topoisomerase poisons and intercalating transcription inhibitors, we also evaluated the cell cycle effects of camptothecin (topoisomerase I),<sup>33</sup> amsacrine, amsacrine-4-carboxamide and mitoxantrone (topoisomerase II),<sup>34,35</sup> actinomycin D, echinomycin, and nogalamycin. We find that the novel diacridines are indeed bisintercalating threading agents, and preliminary data indicate that the DNA complexes of selected members dissociate many orders of magnitude more slowly than those of their monofunctional counterparts. Their cytotoxicity varies markedly with structure. As expected, the known topoisomerase poisons invariably caused G2/M arrest in the cell population tested, whereas the established transcription inhibitors were without effect on cell cycle progression. With the exception of the octamethylene- and piperazine-linked dimers, the dimethylaminoethyl series of diacridines arrest cells in G2/M, suggesting the involvement of topoisomerase poisoning. However, the cycle signature of the former compounds, which are among the most potent of the dimethylaminoethyl dimers, is more akin to that of the transcription inhibitors. Similarly, with the exception of the hexamethylene-linked member, the morpholino dimers fail to perturb the cell cycle distribution, strongly suggesting the lack of involvement of topoisomerase poisoning in their mode of action. Thus, there is a complex cellular response to challenge across the series of threading dimers, the determinants of which are unclear given that the compounds studied appear to bind to DNA by a common mechanism.

**Results**

**Chemistry.** Our approach to the synthesis of bis(9-aminoacrididine-4-carboxamides) is outlined in Schemes 1–3. In short, we first prepared acridone-4-carboxylic acid, converted it to the 9-chloroacrididine-4-acyl chloride, amidated with the carboxamide side chain of choice, and finally coupled two monomers by nucleophilic reaction with bifunctional  $\alpha,\omega$ -diamines.

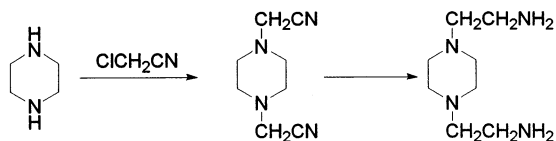
**Scheme 3.** Synthesis of 9-Aminoacrididine-4-carboxamide dimers**Scheme 4.** Synthesis of *o*-Aminoisophthalic acid**Synthesis of 9-Oxoacridan-4-carboxylic Acid.**

The acridone-4-carboxylic acid was prepared via Jourdan–Ullman reaction of *o*-iodoisophthalic acid with aniline to give an *N*-phenylanthranilic acid, which was then cyclized using polyphosphoric acid, yielding 9-oxoacridan-4-carboxylic acid as described by Rewcastle et al.<sup>36</sup> and shown in Scheme 1. This approach was adopted because it can be readily modified to yield 5-substituted acridone-4-carboxylic acids by the use of *o*-substituted anilines: an objective of future work, since substitutions in the 5-position of 9-amino-DACA are known to slow DNA dissociation rates as a result of enhanced chromophore–base pair stacking interactions.<sup>37</sup> *o*-Iodoisophthalic acid was synthesized from *o*-aminoisophthalic acid by diazotization and substitution with iodide according to standard literature methods. *o*-Aminoisophthalic acid is frequently prepared by oxidation of 2-nitro-1,3-xylene, followed by reduction of the nitro group with tin in hydrochloric acid.<sup>38</sup> However, in our hands this method gave poor yields and the workup procedure was difficult. Accordingly, we sought to develop a more efficient route to *o*-aminoisophthalic acid in the current work. Since oxidation of isatin with alkaline hydrogen peroxide is known to give *o*-aminobenzoic acid in good yield,<sup>39</sup> we reasoned that *o*-aminoisophthalic acid could be made by similar treatment of isatin-7-carboxylic acid, which itself can be efficiently prepared by the method of Deady et al.<sup>40</sup> And, indeed, we found that oxidation of isatin-7-carboxylic acid with alkaline hydrogen peroxide (Scheme 4) does give *o*-aminoisophthalic acid in high yield. The advantages of this method include the lack of a need to purify intermediates and the final product, convenience of handling and workup procedures, and high yields.

**Synthesis of 9-Chloroacrididine-4-carboxamides.**

9-Chloro-[*N*-(2-dimethylamino)ethyl]acrididine-4-carboxamide and 9-chloro-*N*-[2-(4-morpholinyl)ethyl]-4-acrididinecarboxamide were prepared from 9-oxoacridan-4-carboxylic acid via 9-chloroacrididine-4-carboxylic acid as described by Atwell et al.<sup>41</sup> Thus, amidation of the acid chloride with an excess of *N,N*-dimethylethylenediamine or *N*-morpholinoethylethylenediamine in anhydrous dichloromethane gave the respective target 9-chloroacrididine-4-carboxamides (Scheme 2). The 9-aminoacrididine-4-carboxamide monomers were prepared from their



**Scheme 5.** Synthesis of 1,4-Bis(aminoethyl)piperazine

corresponding 9-chloro compounds by reacting with ammonia gas in hot phenol solution (Scheme 2).

**Linker Design and Diacridine Synthesis.** With the exception of the C6 compounds (see Figure 1), the linkers were designed to enable the diacridine chromophores to extend over a distance of 10–11 Å and thus span two basepairs in the bisintercalated complex: a geometry known to provide stable bisintercalation.<sup>27</sup> This structural requirement necessitates a linker length of at least seven atoms (Figure 1). Bisintercalation by hexamethylene-linked diacridines is believed to involve a single basepair sandwich complex,<sup>27</sup> although two basepair sandwich models in which the DNA helix is kinked or bent have been mooted.<sup>27</sup> The linkers used here comprise neutral alkyl chains, flexible polyamine chains providing one or two cationic charges at physiological pH, and a semirigid polyamine yielding two net charges for the linker. Most of the  $\alpha,\omega$ -diamines used are available commercially. The tetraamine required for the C6N2 linker was purchased as its tetrahydrochloride salt, basified to the free base, distilled azeotropically with benzene under nitrogen to give the anhydrous agent, and used directly to avoid decomposition. 1,4-Bis(aminoethyl)piperazine, required for the C2pipC2 linker, was prepared from piperazine, as outlined in Scheme 5. Piperazine was reacted with chloroethanenitrile in the presence of sodium carbonate to give piperazino-1,4-bis(ethanenitrile) in quantitative yield.<sup>42</sup> Subsequent reduction of the bis-nitrile with  $\text{LiAlH}_4$  in *N*-ethylmorpholine solution afforded the desired bisamine.<sup>43</sup> The diacridines were finally coupled by following a modified procedure described by Denny et al.,<sup>44</sup> as shown in Scheme 3. The 9-chloroacridine-4-carboxamides were dissolved in phenol and reacted with half a molecular equivalent of the  $\alpha,\omega$ -diamine linkers. After heating at 125 °C for 2 h, and suitable workup, the diacridine free bases were recovered from chloroform and purified by flash chromatography and recrystallization. Their corresponding hydrochloride salts were prepared by treating the free base in methanol with dry hydrogen chloride, followed by precipitation with ethyl acetate.

**DNA Binding.** To establish whether the diacridines bind to DNA by a bisintercalating threading mode, we investigated their capacity to remove and reverse the supercoiling of closed circular pBR 322 DNA as assessed by electrophoretic mobility measurements on agarose gels.<sup>27,45,46</sup> Figure 2 shows typical titration curves for the C8 DMAE, C6N2 DMAE, and C3NC3 morpholino dimers and reveals equivalence binding ratios, where all the supercoiling has been removed and the closed and nicked circular species comigrate, in the range 0.075–0.12 ligand molecules per base pair. Similar titration curves were found for all the compounds studied, and equilibrium dialysis measurements indicate that binding is effectively quantitative at equivalence in these low ionic strength experimental conditions (cation concentration of 30 mM). Since pBR 322 DNA

has 38 negative supercoils at the ionic strength used here,<sup>47,48</sup> and given that removal of each supercoil requires the Watson–Crick duplex to be unwound by 360°, the total amount of helix unwinding per DNA molecule at equivalence is 13 680°. Knowing that pBR 322 has 4362 basepairs, it is a simple matter to calculate the helix unwinding angle per bound ligand molecule from the measured equivalence binding ratios for each of the dimers studied, and these values are given in Table 1. With regard to the dimethylaminoethyl series, helix unwinding angles range from 26° to 46°, which is 1.5–2.7-fold greater than that of the parental monomer, 9-amino-DACA, and confirm that the compounds bind with both of their chromophores simultaneously intercalated (see ref 27). In results to be published elsewhere, the findings for the C6 and C8 DMAE dimers reported here have been corroborated using viscometric titrations with a different plasmid DNA (see ref 27).

The measured helix-unwinding angles reveal linker-dependent variations in duplex winding in the DNA complexes of the dimethylaminoethyl dimers, the unwinding angles for the C8 and C3NC3 linkers being particularly large and that for the C2pipC2 linker being noticeably low. These findings imply the existence of specific interactions between the linker and the DNA base pairs that modify the fine structure of the complexes. A low unwinding angle for simple nonthreading piperazine-containing bisintercalating diacridines has been noted before,<sup>27</sup> which suggests particularly strong interactions between the piperazine ring and the DNA bases. Figure 2 also reveals that the intrinsic electrophoretic mobility of the closed circular DNA diminishes at binding ratios above the equivalence point, where it acquires ligand-induced right-handed supercoils, which is no doubt a consequence of the increase in DNA contour length that accompanies intercalation (see ref 27). This phenomenon is also reflected in the response of the nicked circular species, which behaves hydrodynamically and electrophoretically in a similar way to linear DNA. Thus, the mobility of the nicked circular DNA decreases linearly with increased ligand binding (plot not shown), tending to reach a constant value at about one ligand molecule bound per four basepairs, a value we take as indicative of the stoichiometry of bisintercalative binding. Generally, this plot has a gradient of  $-1$ , an exception being the result for C3NC3 DMAE, where the slope is  $-1.5$ . Taken as a whole, the results of the circular DNA experiments suggest that the dimethylaminoethyl dimers, with the exception of the C6 analogue, bisintercalate forming a “two basepair sandwich” complex, in which the binding site extends over a total of four basepairs, as would be expected given the 10–11 Å length of their linkers (Figure 1). The helix unwinding angle for the C6 DMAE dimer is consistent with a bithreading mode of binding, but its linker, at 8.8 Å, is too short on the basis of modeling to allow bisintercalation without severe bending of the DNA helix in the complex. Alternatively, it may bisintercalate sandwiching only one basepair, thereby violating the neighbor-exclusion principle.<sup>27</sup> Either way, the structure of its DNA complex, while bisintercalated, is necessarily different from those of its congeners.

The lower basicity of the morpholino group, whose  $pK$  lies between 7 and 8,<sup>41</sup> leads to only partially charged

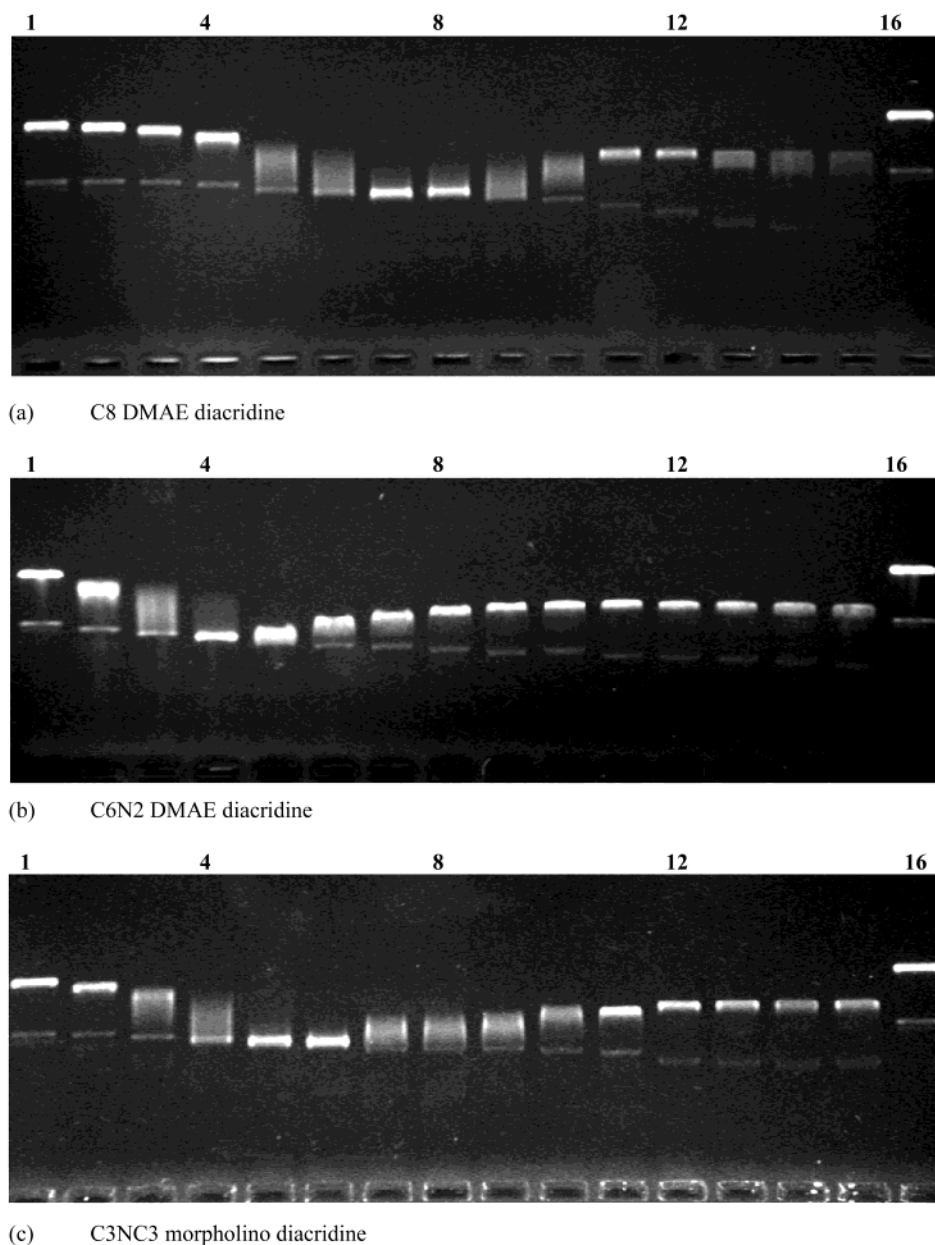


**Figure 2.** Effects of the C8 DMAE, C6N2 DMAE, and C3NC3 morpholino threading diacridines on the supercoiling of pBR 322 DNA. Measurements were made in 40 mM Tris-acetate buffer, pH 7.5 on 0.8% agarose gels electrophoresed for 75 min at 5 V/cm. Drug to DNA ratios in lanes 1–16 for C8 DMAE are 0, 0.01, 0.02, 0.03, 0.04, 0.05, 0.06, 0.07, 0.08, 0.09, 0.10, 0.15, 0.20, 0.25, 0.30, and 0. Drug to DNA ratio in lanes 1–16 for C2N6 DMAE and C3NC3 morpholino are 0, 0.04, 0.06, 0.08, 0.10, 0.12, 0.14, 0.16, 0.18, 0.20, 0.25, 0.30, 0.35, 0.40, 0.50, and 0.

side chains for the morpholino dimers at pH 7.5. One consequence of this is that the circular DNA complexes of the alkyl- and C2pipC2-linked morpholino dimers appeared to partly dissociate on agarose gels under the standard experimental conditions used here. Accordingly, the helix unwinding angles for these three compounds were determined at pH 6.1, where their DNA complexes are stable to electrophoresis. In contrast, the remaining morpholino dimers, linked by charged linear amines, appeared stable to electrophoresis at the higher pH. The results of the superhelical titrations for the morpholino compounds are included in Table 1 and also confirm this series of novel diacridines as bisintercalating agents that, with the exception of the C6 dimer, have helix-unwinding angles ranging from 27° to 33°. However, in distinction to the findings with the dimethylaminoethyl series, the mea-

sured unwinding angles are largely independent of linker structure, which implies that the acridine chromophore and its pendant side chain is the most dominant determinant of helical winding in bisintercalated complexes of the morpholino dimers. Notwithstanding this generalization, the piperazine-linked compound remains an exception, with a low unwinding angle, indistinguishable from that of its dimethylaminoethyl analogue. The C6 dimer has an unwinding angle closer to the value of its monofunctional parent, suggesting either a highly strained bisintercalated complex or that the ligand binds in a mixed monofunctional-bifunctional mode.

In preliminary kinetic studies using the surfactant sequestration method (see refs 15–20) to measure the rates of dissociation of calf thymus DNA complexes of selected threading dimers and actinomycin, we found

**Table 1.** Cytotoxicity and Helix-Unwinding Angles for the Compounds Studied<sup>b</sup>

agent	cytotoxicity IC <sub>50</sub> (nM)	equivalence binding ratio	helix unwinding angle, deg
Topoisomerase Poisons			
mitoxantrone	3.6 ± 1.3		18 <sup>a</sup>
amsacrine	130 ± 39		21 <sup>b</sup>
amsacrine-4-carboxamide	120 ± 20		25 <sup>c</sup>
camptothecin	5.3 ± 1.5	NA	NA
Transcription Inhibitors			
actinomycin D	1.6 ± 1.0		18 <sup>d</sup>
echinomycin	0.5 ± 0.1		48 <sup>e</sup>
nogalamycin	59 ± 19		12 <sup>d</sup>
chromomycin	3.5 ± 0.7	NA	NA
DMAE Diacridines			
DMAE monomer	120 ± 25		17 <sup>f</sup>
C6 DMAE	87 ± 6	0.090 ± 0.010	36 ± 3
C8 DMAE	35 ± 5	0.075 ± 0.005	43 ± 2
C3NC3 DMAE	50 ± 14	0.070 ± 0.005	46 ± 2
C3NC4 DMAE	250 ± 36	0.110 ± 0.010	30 ± 2
C6N2 DMAE	590 ± 55	0.090 ± 0.050	36 ± 2
C2pipC2 DMAE	63 ± 2	0.125 ± 0.010	26 ± 3
Morpholino Diacridines			
morpholino monomer	3800 ± 60		18 <sup>f</sup>
C6 morpholino	710 ± 110	0.145 ± 0.015	22 ± 2 <sup>g</sup>
C8 morpholino	810 ± 180	0.110 ± 0.010	30 ± 2 <sup>g</sup>
C3NC3 morpholino	47 ± 10	0.112 ± 0.014	29 ± 3
C3NC4 morpholino	75 ± 25	0.100 ± 0.010	33 ± 3
C6N2 morpholino	710 ± 61	0.100 ± 0.015	33 ± 4
C2pipC2 morpholino	290 ± 150	0.120 ± 0.010	27 ± 2 <sup>g</sup>

<sup>a</sup> Data taken from ref 53. <sup>b</sup> Data taken from ref 54. <sup>c</sup> Data taken from ref 20. <sup>d</sup> Data taken from ref 55. <sup>e</sup> Data taken from ref 9. <sup>f</sup> Data taken from ref 41. <sup>g</sup> Measurements made at pH 6.1. <sup>h</sup> Cytotoxicity was measured after 72 h incubation with CCRF-CEM human leukemia cells. Helix unwinding angles were measured by agarose gel electrophoresis using pBR322 covalently closed circular DNA at pH 7.5. Equivalence binding ratios are expressed in basepair units. NA, not applicable.

**Table 2.** Dissociation Kinetics for Calf Thymus DNA Complexes of Selected Agents Studied<sup>a</sup>

compd	dissociation time constants, s		
	τ <sub>1</sub>	τ <sub>2</sub>	τ <sub>3</sub>
C8 DMAE	5	17	53
C3NC3 DMAE	6	32	130
C3NC3 morpholino	5	30	88
C6N2 DMAE	6	33	180
C2PipC2 DMAE	7	22	220
actinomycin	19	68	790

<sup>a</sup> A 900 μL portion of a DNA–ligand complex solution comprising 555 μM DNA in base pairs and 55 μM ligand in 0.1 SHE buffer was mixed with 100 μL of 200 mM SDS solution in 0.1 SHE buffer in a 1 mL semi-micro-quartz cuvette at 23 °C. Data were collected on a Cary 50 spectrophotometer at wavelengths of 423 nm for the bis(9-aminoacridine-4-carboxamides) and 430 nm for actinomycin D. Reaction progress curves were deconvoluted into three exponentials using the Levenberg–Marquardt algorithm in the Origin v 7.0 software package.

that the complexes dissociate by a complex mechanism involving four discernible steps, three of which can be captured by a manual mixing technique (Table 2). The rapid, missing component accounts for about one-third of the total reaction in buffer of ionic strength 0.1 at 23 °C. Under these conditions, actinomycin dissociates from DNA with resolvable time constants of 19, 69, and 790 s, and the C8 DMAE diacridine dissociates with time constants of 5, 17, and 53 s. Taking into consideration the relative amplitudes of the individual transients (data not shown), the weighted mean dissociation rate of the DNA complex of the C8 DMAE dimer is approximately 6-fold faster than that of actinomycin.

Adding a single positive charge to the linker of the bithreading agent slows average dissociation rates approximately 2-fold in both the dimethylaminoethyl and morpholino series (Table 2), and a second positive charge slows dissociation yet further (Table 2). These preliminary findings, when compared with complex lifetimes in the range 0.1–0.4 s for 9-amino-DACA and the C8-linked nonthreading diacridine,<sup>17,44</sup> illustrate the profound slowing effect imparted by the threading mechanism when set in a bisintercalating binding mode.

**Cytotoxicity.** The relationships between cytotoxicity and structure for the threading diacridines were explored using a conventional growth inhibition assay with CCRF-CEM human leukemia cells. For the purposes of comparison, we also investigated the cytotoxicity of the topoisomerase II poisons mitoxantrone, amsacrine, and amsacrinecarboxamide;<sup>1–3,20,34,35</sup> the topoisomerase I poison camptothecin;<sup>33</sup> the intercalating transcription inhibitors actinomycin D, echinomycin, and nogalamycin;<sup>8–10,13–16</sup> and the minor groove binding transcription inhibitor chromomycin.<sup>49</sup> Among the topoisomerase poisons, the anilinoacridines amsacrine and amsacrinecarboxamide have similar IC<sub>50</sub> values in the range 120–130 nM, whereas mitoxantrone and camptothecin are some 25-fold more potent (Table 1). With the exception of nogalamycin, whose IC<sub>50</sub> is 59 nM, the transcription inhibitors exhibited IC<sub>50</sub> values of approximately 1 nM. In respect of the monofunctional parents of the threading dimers, the toxicity of 9-amino-DACA is indistinguishable from that of the anilinoacridines, which accords with its known ability to poison topoisomerase II,<sup>5,6</sup> whereas the morpholino analogue is 30-fold less potent, consistent with previous findings in other cell lines.<sup>41</sup> In the dimethylaminoethyl dimer series, the C6-, C8-, C3NC3-, and C2pipC2-linked compounds are more potent than 9-amino-DACA, by about 2–3-fold on average, whereas the C3NC4 and C6N2 dimers are 2- and 5-fold less active, respectively. Thus, for the dimethylaminoethyl side chain, dimerization can enhance or diminish biological activity, depending on the nature of the linker. In contrast, dimerization in the morpholino series consistently enhances cytotoxicity, in the case of the C3NC3- and C3NC4-linked dimers, bringing potency into the same range as that exhibited by their dimethylaminoethyl homologues. Thus, the most active morpholino dimers are some 50–80-fold more potent than their parental monomer. For both the dimethylaminoethyl and the morpholino dimers, varying the linker alters cytotoxicity by more than an order of magnitude. The C3NC3 linker confers high potency on both groups of compounds tested, but otherwise different groups, for example, C8 and C2pipC2 in the case of the dimethylaminoethyl dimers, are also associated with high cytotoxicity. Overall, neither the dimethylaminoethyl series nor the morpholino series of dimers is conspicuously more toxic than the other.

**G2/M Arrest.** Flow cytometric analysis was specifically undertaken to assess the impact of the threading dimers on cell cycle progression. However, the respective analyses also provide information, from detection of cells having less than G1 DNA content, on occurrence of cell death, and this matter will be considered separately. Flow cytometry was performed after incubation for 24 and 48 h in the presence of agents at concentrations



**Table 3.** Effects of Compounds Studied on Proportion (%) of CCRF-CEM Cells at G2/M Determined by Flow Cytometry

compound	24 h			48 h			G2/M arrest <sup>c</sup>
	1 <sup>x</sup> <sup>b</sup>	2 <sup>x</sup>	10 <sup>x</sup>	1 <sup>x</sup>	2 <sup>x</sup>	10 <sup>x</sup>	
Topoisomerase Poisons							
mitoxantrone	32	53	83	24	32	50	yes: 2 <sup>x</sup>
amsacrine	51	47	57	35	d	52	yes: 1 <sup>x</sup>
amsacrine-4-carboxamide	83	73	d	35	42	d	yes: 1 <sup>x</sup>
camptothecin	29	48	d	31	47	d	yes: 2 <sup>x</sup>
Transcription Inhibitors <sup>a</sup>							
actinomycin D	21	20	28	20	22	11	no
DMAE Diacridines							
DMAE monomer	20	30	61	18	22	53	yes: 10 <sup>x</sup>
C6 DMAE	17	34	34	12	43	39	yes: 2 <sup>x</sup>
C8 DMAE	20	23	29	17	21	21	no
C3NC3 DMAE	20	19	44	19	20	46	yes: 10 <sup>x</sup>
C3NC4 DMAE	19	30	52	14	25	81	yes: 10 <sup>x</sup>
C6N2 DMAE	19	25	61	16	16	69	yes: 10 <sup>x</sup>
C2pipC2 DMAE	18	18	20	21	19	20	no
Morpholino Diacridines							
morpholino monomer	17	17	21	10	18	18	no
C6 morpholino	25	29	38	23	25	44	yes: 10 <sup>x</sup>
C8 morpholino	19	19	24	14	17	24	no
C3NC3 morpholino	18	15	13	12	12	13	no
C3NC4 morpholino	17	15	17	11	13	11	no
C6N2 morpholino	24	27	24	24	27	23	no
C2pipC2 morpholino	27	24	28	23	22	23	no

<sup>a</sup> Data for transcription inhibitors echinomycin D, nogalamycin, and chromomycin have been omitted since the findings were as shown for actinomycin D (no variation from control). <sup>b</sup> Cells were incubated for 24 or 48 h in the presence of the compound shown at concentrations equal to the IC<sub>50</sub> (see Table 1) or at two or 10 times that concentration, control preparations being left untreated. No consistent differences between 24 and 48 h control values were evident (total = 44 determinations), the G2/M proportion being almost always in the range 17–22% and never more than 25%. <sup>c</sup> Occurrence of G2/M arrest was arbitrarily determined on the basis of the G2/M proportion being 40% or more. <sup>b</sup> Occurrence of cell death at a level sufficient to preclude identification and computation of any G2/M peak in the flow cytometric profile.

ranging from the IC<sub>50</sub> (based on 72 h incubation), upward to two, five, or 10 times that level. It was readily apparent, with respect to both the established drugs employed for control purposes and also for the novel agents under test, that when treatment-related alteration of the flow cytometric profile did occur, the pattern was consistent. Such change invariably involved an increase in the proportion of cells at G2/M, and when observed, accumulation was typically time- and concentration-dependent within the limitations of the parameter selected for study. Thus, to facilitate data presentation, we have focused on the proportion of cells at G2/M, respective values being adopted after reviewing each profile and confirming that the numeric value computed is identifiable with an evident “peak”. If no such peak was apparent, a scenario most often synonymous with cell death and complete loss of the typical profile, no value was adopted for “percentage of cells in G2/M”. Otherwise, G2/M arrest was deemed to have occurred if the result was more than 40%, which compares with a value of about 21% consistently observed in preparations of cells not subject to drug treatment.

The topoisomerase poisons mitoxantrone and camptothecin and the amsacrine-related agents all caused G2/M arrest by the standard adopted (see Figure 1c of the Supporting Information and Table 3). These agents exhibit the effect at relatively low concentrations, typically one or two times the IC<sub>50</sub> values, and G2/M arrest is readily evident after incubation for 24 h. This

response is clearly distinguished from that obtained using the transcription inhibitors actinomycin D, chromomycin, echinomycin, and nogalamycin (Table 3), for which there was no evidence for accumulation of cells in G2/M. With regard to the threading dimethylaminoethyl dimers, the parental monomer, 9-amino-DACA, consistently caused G2/M arrest, but at generally higher doses than required for the other topoisomerase poisons (Table 3). With respect to the novel agents, two response patterns were observed: either G2/M arrest or no effect on cell cycle distribution. Typical flow cytometric profiles are shown in Figure 1 of the Supporting Information, and the data for all the agents studied are summarized in Table 3. With the exception of the C8 and C2pipC2 members, which appear to have no impact on cell cycle distribution, the dimethylaminoethyl dimers caused G2/M arrest, at least when they were assessed at high concentrations (Figure 1a of the Supporting Information, Table 3). The results at lesser concentrations typically indicate an increase in the proportion of cells at G2/M, but not to the extent of reaching the arbitrary level adopted on the basis of the established topoisomerase poisons. In every case, increasing the concentration of the agent enhanced, or at least maintained, the size of the G2/M peak, in a manner similar to that found for 9-amino-DACA. By contrast, the behavior of the morpholino-based agents is generally quite different. The monomer and all the dimers, with the exception of the C6-linked member, showed no discernible effect on cell cycle distribution under the conditions employed in these studies (Figure 1b of the Supporting Information, Table 3). Accumulation of cells in G2/M was observed using the C6 morpholino dimer at the highest concentration tested.

**Kinetics of Cell Death.** In the course of the flow cytometric analyses summarized in Table 3, we were able to discern accumulation of cells having less than G1 DNA content in some instances. Although the flow cytometric studies involved equitoxic concentrations based on 72 h incubation, it was evident that the appearance of dead cells at earlier times was nonrandomly associated with particular agents. By the “sub-G1 DNA peak” criterion, death of the entire cell population after incubation for 24 or 48 h was only observed with the recognized topoisomerase poisons amsacrine, amsacrine-4-carboxamide, and camptothecin. These results were as expected, insofar as the effect was observed at the highest concentration employed (10 times), and was more marked after 48 h than at 24 h. “Early death” results obtained with the transcription inhibitors chromomycin, echinomycin, actinomycin D, and nogalamycin were similar to those found for the threading dimers and mitoxantrone. In these cases, with the exception of the amine-linked morpholino dimers, some cell death was evident in all instances, at least using the highest concentration of the agent after incubation for 48 h, but DNA profiles were never distorted beyond recognition. The amine-linked morpholino dimers, along with 9-amino-DACA, appear not to induce evident cell death following exposure of CCRF-CEM cells for up to 48 h.

## Discussion

**DNA Binding and Cytotoxicity.** In this work we have designed and synthesized a series of bis(9-ami-

noacridine-4-carboxamides) and shown that they bisintercalate into DNA via a threading mode, whereby the carboxamide side chains come to lie in one groove of the DNA and the linker lies in the other. Preliminary kinetic studies with selected members indicate that the dimers dissociate orders of magnitude more slowly from DNA than simple nonthreading diacridines, as postulated, which implies the involvement of the carboxamide side chains in interactions with the DNA bases. Additional NMR or crystallographic studies are required to establish that these interactions are with guanines, as anticipated. Notwithstanding the fact that the threading dimers share a common mode of binding, the relationships between cytotoxicity, ligand structure, and helix unwinding are complex, allowing few, if any, generalizations to be made across the group as a whole. Rather, the various subgroups must be considered. Thus, among members of the dimethylaminoethyl series, the most active compounds are the C8-, C3NC3-, and C2pipC2-linked dimers which are two to three times more potent than 9-amino-DACA and, respectively, have a neutral, a flexible singly charged, and a semirigid doubly charged linker, indicating biological efficacy across a wide range of linker types (Table 1). However, that subtle structural features are important is made clear by the finding that adding a single methylene group to the C3NC3 linker, to give C3NC4, lowers toxicity 5-fold and removing the ethyl cross-link from C2pipC2 to give the flexible C6N2 linker suppresses it by an order of magnitude. In addition, dichotomies are found when comparing helix-winding effects with cytotoxicity data, which are best illustrated by the observation that the C8 and C3NC3 dimers have the highest unwinding angles, 43° and 46°, whereas C2pipC2 has the lowest, 26°. When considering the morpholino series, we found, as noted by Atwell et al.,<sup>41</sup> that the parental monomer is much less cytotoxic than 9-amino-DACA. However, when incorporated into threading dimers, the cytotoxicity of the resulting bismorpholino compounds is substantially enhanced in a manner dependent on linker structure, the singly charged amine linkers C3NC3 and C3NC4 having potencies comparable to those of the most active members of the dimethylaminoethyl series. Adding an additional charge, making the linker neutral, or making it more rigid all compromise cytotoxicity (Table 1). Resolving these difficulties in understanding the structure–activity relationships for the bis(9-aminoacridine-4-carboxamides) is made more complex by the finding that the dimers engage apoptosis by at least two distinct mechanisms, as discussed below.

#### G2/M Arrest and the Mechanism of Cell Death.

The mechanism of action of cytotoxic drugs most commonly involves perturbations to DNA synthesis, transcription, or mitosis, the disruption of any of these processes being sufficient to induce apoptosis in susceptible cells. The requisite signaling pathway following formation of the critical drug–target complex has proven difficult to elucidate for cytotoxins in general and specially so for transcription template inhibitors such as actinomycin D, because these drugs are often used as “tools” for dissecting such pathways by establishing a requirement for transcription in particular contexts. Likewise, the pathways between disruption of topoisomerase function and associated DNA damage on one

hand and caspase activation as initiating apoptosis on the other have not been defined<sup>3</sup>. Critical to such pathways is disruption of cell cycle progression and the adequacy, or otherwise, of cell cycle checkpoints.<sup>50</sup> It is logical, therefore, that processes associated with topoisomerase function, cell cycle arrest, and apoptosis induction, be specifically viewed as focal points for cancer drug development.<sup>51</sup> The observations recorded here, however, indicate that direct and causal relationships between various steps triggered by drug–target interaction are not invariably observed. While the sequence drug–target interaction, cell cycle arrest, and cell death could be delineated in relation to the recognized topoisomerase poisons used, this sequence varied and/or was only partially exhibited by the bis(9-aminoacridine-4-carboxamides) and the established transcription inhibitors.

In common with etoposide,<sup>32</sup> G2/M arrest of CCRF-CEM cells was readily evident within 24 h of exposure to mitoxantrone, amsacrine, amsacrine-4-carboxamide, and camptothecin, a pattern of response that distinguished these agents from the known transcription inhibitors used (Table 3). Although G2/M arrest is commonly observed in response to a range of DNA-damaging drugs, the poisoning of topoisomerase II is well-recognized to precipitate such an event,<sup>30</sup> which accords with our findings. In contrast, the recognized transcription inhibitors and the bisintercalating morpholino dimer series (with the exception of the C6-member, whose DNA complex, as illustrated by its low helix unwinding angle, is somewhat different to those of its longer homologues) fail to arrest cells in G2/M. This necessarily means these agents engage apoptosis by a different mechanism than the topoisomerase poisons, and this finding may be taken to imply that the morpholino dimers, by analogy to the transcription template inhibitors and consistent with their design principles, are cytotoxic as a consequence of inhibiting transcription. The situation with the dimethylaminoethyl dimers and cycle progression is more complex. With the exception of the C8- and the C2pipC2-linked DMAE ligands, these agents arrest cells in G2/M in a manner similar to the recognized topoisomerase poisons, which suggests the involvement of topoisomerase activity in their mechanism of action. By analogy, this finding also implies that the C8 DMAE and C2pipC2 DMAE dimers engage apoptosis through a transcription-initiated pathway, in a manner similar to the morpholino series. To substantiate this conclusion we have begun studies of the effects of the bis(9-aminoacridine-4-carboxamides) on global gene expression using DNA microarrays. The preliminary data are limited but indicate that, as a class, these agents profoundly perturb gene expression, with the concentration of many transcripts being diminished, while the concentration of others is enhanced. Clearly, further studies are needed, both with the established template inhibitors and the most toxic of the threading dimers, to elucidate relationships between ligand structure, gene expression, topoisomerase poisoning, cycle arrest, and apoptosis.

#### Conclusions

In summary, our findings show that both the dimethylaminoethyl and morpholino dimer series bisinter-



calate into DNA by a threading mode, in which they place the 4-carboxamide side chain in one groove, and the interchromophore linker in the other. The compounds appear to have binding sites extending over four basepairs in which the middle two are sandwiched by the acridine chromophores. This binding mode results in a substantial slowing of dissociation rates, as indicated by preliminary kinetic findings, so that the lifetimes of the bisintercalated complexes begin to approach those of known template transcription inhibitors. However, despite common structural features, cytotoxicity varies markedly within both the dimethylaminoethyl and the morpholino series, depending on linker type, although potency is similar for the most active compounds in each class. The latter, with IC<sub>50</sub> values around 50 nM, are C8 DMAE, C3NC3 DMAE, C2pipC2 DMAE, C3NC3 morpholino, and C3NC4 morpholino. With the exception of C3NC3 DMAE, none of these compounds, in common with established transcription inhibitors, perturb cell cycle progression, from which we infer that their mechanism of action does not involve poisoning of topoisomerases. By contrast, C3NC3 DMAE, like established topoisomerase poisons, causes cells to arrest in G2/M, which we take to imply at least partial involvement of topoisomerase poisoning in its mode of action. Thus, specifically in relation to the most cytotoxic compounds, the common mode of bisintercalation evokes complex cellular responses that vary according to side chain and linker structure. A detailed explanation for the manner in which particular structural features determine response patterns and ultimate toxicity is not available. However, the extent to which apparently minor structural change perturbs toxicity encourages evaluation of more members of this class of agent in order to explore more fully their pharmacological potential.

## Experimental Section

**Chemistry.** Melting points were measured on a Reichert "thermopan" microscope hot-stage apparatus up to 300 °C and are recorded uncorrected. Microanalyses were performed by the Microanalytical Unit, Australian National University, Canberra, Australia. NMR spectra were recorded on a Bruker AM-300 spectrometer operating at 300.17 and 75.48 MHz for <sup>1</sup>H and <sup>13</sup>C, respectively. Chemical shifts are reported as  $\delta$  values in ppm relative to internal tetramethylsilane. The solvent was deuterated chloroform, unless otherwise specified. DEPT-135 was used to identify proton-bound carbon atoms in <sup>13</sup>C NMR spectra. MALDI-TOF mass spectra were obtained using a hydroxycinnamic acid matrix on a PerSeptive Biosystems Voyager mass spectrometer. All solvents were laboratory grade and used without further purification unless otherwise stated. Phenol was redistilled and kept under nitrogen in the dark. Dichloromethane was stored over anhydrous calcium chloride, refluxed for 4 h, and then distilled and stored over 4A molecular sieves. All chemical reagents were used as obtained from commercial suppliers without further purification unless otherwise indicated.

**Isatin-7-carboxylic Acid.** A solution of methyl anthranilate (31.5 g, 0.21 mol), chloral hydrate (35.0 g, 0.21 mol), and hydroxylamine hydrochloride (28.6 g, 0.41 mol) in concentrated sulfuric acid (25 g) and water (1.4 l) was heated at 95 °C with stirring for 10 min and then kept at 4 °C for 16 h. The precipitate that formed on cooling was collected by filtration, washed with cold water, and dried. Methyl 2-[(hydroxyimino)acetyl]amino}benzoate was obtained as a cream-colored solid (31.2 g, 67% yield), mp 174–175 °C (lit.<sup>52</sup> mp 180 °C). This intermediate was used in the next step

without further purification, where portions of it were added over 40 min (total, 15.0 g, 67.5 mmol) to a stirred solution of concentrated sulfuric acid (75 g) at 60–65 °C. The resulting mixture was heated at 95 °C for 1 h and then poured into ice-water after being cooled. The precipitate that formed was filtered off and dissolved in 1 M sodium hydroxide, and insoluble material was removed by filtration. The filtrate was then acidified with concentrated hydrochloric acid to pH 2, and the solid that precipitated filtered off, washed with cold water, and dried. Isatin-7-carboxylic acid was obtained as an orange solid (10.1 g, 78%), mp 274–275 °C, (lit.<sup>52</sup> mp 276–277 °C).

***o*-Aminoisophthalic Acid.** Isatin-7-carboxylic acid (9.55 g, 50 mmol) was treated with 3% hydrogen peroxide (200 mL) and 10% sodium hydroxide (200 mL). The resulting mixture was stirred at room temperature for 2 h and then acidified with concentrated hydrochloric acid to pH 2. The precipitate that formed was collected by filtration, washed with cold water, and dried. The product was obtained as a yellow solid (6.60 g, 73%), mp 226–227 °C (from acetic acid), (lit.<sup>38</sup> mp 227–228 °C). <sup>1</sup>H NMR (DMSO-*d*<sub>6</sub>): 6.57 (t, 1H, *J* = 7.8 Hz, H-5), 8.00 (d, 2H, *J* = 7.8 Hz, H-4 and H-6).

***o*-Iodoisophthalic Acid.** *o*-Iodoisophthalic acid was prepared according to literature procedures,<sup>40</sup> mp 239–240 °C (lit.<sup>40</sup> mp 240–241 °C). <sup>1</sup>H NMR (DMSO-*d*<sub>6</sub>): 7.06 (t, 1H, *J* = 7.9 Hz, H-5), 7.89 (d, 2H, *J* = 7.9 Hz, H-4 and H-6), 11.51 (br s, 2H, 2CO<sub>2</sub>H).

**2-(Phenylamino)isophthalic Acid.** This compound was made by Jourdan–Ullman reaction of the *o*-iodoisophthalic acid and aniline as previously described,<sup>40</sup> mp 250–251 °C (lit.<sup>40</sup> mp 247–248 °C). <sup>1</sup>H NMR (DMSO-*d*<sub>6</sub>): 6.85–6.90 (m, 3H, 3ArH), 6.99 (t, 1H, *J* = 7.9 Hz, ArH), 7.18 (t, 2H, *J* = 7.7 Hz, 2ArH), 7.91 (d, 2H, *J* = 7.9 Hz, 2ArH), 9.62 (br s, 1H, NH), 12.94 (br s, 2H, 2CO<sub>2</sub>H).

**9-Oxoacridan-4-carboxylic Acid.** Cyclization of the above 2-(phenylamino)isophthalic acid in polyphosphoric acid at 120 °C gave the title product as a yellow solid, mp >300 °C (lit. mp 324–325 °C). <sup>1</sup>H NMR (DMSO-*d*<sub>6</sub>): 7.29–7.36 (m, 2H, 2ArH), 7.74–7.76 (m, 2H, 2ArH), 8.22 (d, 1H, *J* = 8.3 Hz, ArH), 8.42 (d, 1H, *J* = 7.1 Hz, ArH), 8.51 (d, 1H, *J* = 7.9 Hz, ArH), 11.93 (s, 1H, NH).

**9-Chloroacridine-4-carbonyl Chloride.** This intermediate was prepared from 9-oxoacridan-4-carboxylic acid by following the literature procedure of Atwell et al.,<sup>41</sup> and was used in the next step without further purification.

***N*-[2-(*N*-Morpholino)ethyl]-9-chloroacridine-4-carboxamide.** An ice-cold solution of 4-aminoethylmorpholine (4.88 g, 37.5 mmol) in dichloromethane (10 mL) was added over 5 min to a stirred suspension of the above carbonyl chloride (7.5 mmol) in dichloromethane (10 mL) cooled on ice. The resulting solution was stirred at room temperature for 2 h, washed twice with 10% sodium carbonate and then with brine, and finally dried over sodium sulfate. Removal of the solvent in vacuo gave the product as a yellow solid (2.73 g), which was recrystallized from benzene/petroleum ether as a yellow powder (2.27 g, 82%), mp 123–124 °C. <sup>1</sup>H NMR: 2.63–2.66 (m, 4H, 2CH<sub>2</sub>), 2.79 (t, 2H, *J* = 6.2 Hz, CH<sub>2</sub>), 3.80–3.86 (m, 6H, 3CH<sub>2</sub>), 7.69–7.79 (m, 2H, 2ArH), 7.89 (dt, *J* = 6.8, 1.5 Hz, ArH), 8.34 (d, 1H, *J* = 8.5 Hz, ArH), 8.47 (d, 1H, *J* = 8.3 Hz, ArH), 8.63 (dd, 1H, *J* = 8.5, 1.5 Hz, ArH), 9.01 (dd, 1H, *J* = 6.8, 1.5 Hz, ArH), 11.83 (br s, 1H, CONH).

***N*-[2-(*N*-Dimethylamino)ethyl]-9-chloroacridine-4-carboxamide.** The title compound was prepared from the above carbonyl chloride and *N,N*-dimethylethylenediamine, in the same manner as *N*-[2-(*N*-morpholino)ethyl]-9-chloroacridine-4-carboxamide and was used in following steps without further purification. <sup>1</sup>H NMR: 1.34 (s, 6H, N(CH<sub>3</sub>)<sub>2</sub>), 1.61 (t, 2H, *J* = 5.7 Hz, CH<sub>2</sub>), 2.68 (q, 2H, *J* = 5.7 Hz, CH<sub>2</sub>), 6.54–6.62 (m, 2H, 2ArH), 6.73 (t, 1H, *J* = 6.4 Hz, ArH), 7.08 (d, 1H, *J* = 8.2 Hz, ArH), 7.27 (d, 1H, *J* = 8.5 Hz, ArH), 7.42 (dd, 1H, *J* = 8.2, 1.5 Hz, ArH), 7.86 (dd, 1H, *J* = 6.4, 1.1 Hz, ArH), 10.76 (s, 1H, CONH).

***N*-[2-(*N*-Morpholino)ethyl]-9-aminoacridine-4-carboxamide.** Dry ammonia gas was bubbled through a solution of *N*-[2-(*N*-morpholino)ethyl]-9-chloroacridine-4-carboxamide (0.37

g, 1.0 mmol) in anhydrous phenol (3 g) at 115 °C for 30 min. After cooling, the reaction mixture was stirred with 20% sodium hydroxide (20 mL), and the resulting suspension was extracted with chloroform. The organic extract was then washed with saturated sodium carbonate and dried over sodium sulfate. Evaporation of the solvent gave the 9-amino compound, which was recrystallized from benzene/petroleum ether as a yellow solid in 96% yield. <sup>1</sup>H NMR: 2.62–2.65 (m, 4H, 2CH<sub>2</sub>), 2.78 (t, 2H, *J* = 6.0 Hz, CH<sub>2</sub>), 3.79–3.83 (m, 6H, 3CH<sub>2</sub>), 6.05 (br s, 2H, NH<sub>2</sub>), 7.31–7.41 (m, 2H, 2ArH), 7.70 (t, 1H, *J* = 7.5 Hz, ArH), 7.93 (d, 1H, *J* = 8.5 Hz, ArH), 8.01–8.05 (m, 2H, 2ArH), 8.82 (d, 1H, *J* = 6.8 Hz, ArH), 12.61 (br s, 1H, CONH). The di-hydrochloride salt of this product was prepared by treating its methanol solution with hydrogen chloride gas followed by precipitation with ethyl acetate to give a yellow solid, mp 283–284 °C, (lit.<sup>41</sup> mp 282–284 °C).

***N*-[2-(*N*-Dimethylamino)ethyl]-9-aminoacridine-4-carboxamide (9-amino-DACA).** The title compound was prepared in 77% yield from its corresponding 9-chloro precursor as a yellow solid, by the procedure used to make the morpholino derivative described above. Its dihydrochloride salt was obtained as a yellow solid, mp 288–290 °C (lit.<sup>41</sup> mp 292–293 °C).

**C8-DMAE Dimer: General Procedure for Synthesis of Diacridines.** A mixture of *N*-[2-(*N*-dimethylamino)ethyl]-9-chloroacridine-4-carboxamide (0.35 g, 1.0 mmol), 1,8-diaminooctane (72 mg, 0.50 mmol), and phenol was heated at 125 °C with stirring for 2 h. After cooling, the reaction mixture was added to a large excess of diethyl ether and the organic solution decanted. The residue was washed with diethyl ether and dissolved in 0.5 M hydrochloric acid, and insoluble material was removed by filtration. The filtrate was then basified with 10% sodium hydroxide and extracted twice with chloroform. The combined organic extracts were washed with 10% sodium carbonate and brine and dried over sodium sulfate. Evaporation of the solvent gave the product as an orange oil which solidified gradually. The solid was recrystallized from methanol and then flash chromatographed on alumina (ethyl acetate then methanol/chloroform (*v/v* = 1/1)) to yield a yellow solid in 55% yield, mp 92 °C. Found: C, 70.94; H, 7.39; N, 14.80. C<sub>44</sub>H<sub>54</sub>N<sub>8</sub>O·H<sub>2</sub>O requires: C, 70.94; H, 7.58; N, 15.04. <sup>1</sup>H NMR: 1.25–1.32 (m, 8H, 4CH<sub>2</sub>), 1.69 (m, 4H, 2CH<sub>2</sub>), 2.40 (s, 12H, 2N(CH<sub>3</sub>)<sub>2</sub>), 2.68 (t, 4H, *J* = 6.1 Hz, 2CH<sub>2</sub>), 3.75 (q, 8H, *J* = 6.1 Hz, 4 CH<sub>2</sub>), 5.29 (br s, 2H, 2NH), 7.33–7.41 (m, 4H, 4ArH), 7.68 (t, 2H, *J* = 7.5 Hz, 2ArH), 8.04 (d, 4H, *J* = 8.7 Hz, 4ArH), 8.17 (d, 2H, *J* = 8.5 Hz, 2ArH), 8.85 (d, 2H, *J* = 6.8 Hz, 2ArH), 12.53 (br s, 2H, 2CONH). <sup>13</sup>C NMR: 26.5 (2CH<sub>2</sub>), 28.9 (2CH<sub>2</sub>), 31.5 (2CH<sub>2</sub>), 37.9 (2CH<sub>2</sub>), 45.4 (2N(CH<sub>3</sub>)<sub>2</sub>), 50.9 (2CH<sub>2</sub>), 58.3 (2CH<sub>2</sub>), 115.6 (2C), 116.4 (2C), 122.0 (2CH), 122.3 (2CH), 123.3 (2CH), 126.4 (2CH), 128.3 (2C), 129.5 (2CH), 130.4 (2CH), 134.4 (2CH), 147.2 (2C), 147.9 (2C), 152.4 (2C), 166.4 (2C). MALDI-MS: 727.0 (M + 1). Its tetrahydrochloride salt was obtained as a yellow solid, mp 186–188 °C. The following diacridines were prepared in a similar way.

**C6-morpholino Dimer.** This was prepared as for the C8-DMAE dimer, from *N*-[2-(*N*-morpholino)ethyl]-9-chloroacridine-4-carboxamide and hexamethylenediamine, and then recrystallized from ethyl acetate as a yellow solid (75% yield), mp 200–202 °C. Found: C, 69.17; H, 6.74; N, 13.99. C<sub>46</sub>H<sub>54</sub>N<sub>8</sub>O<sub>4</sub>·H<sub>2</sub>O requires: C, 68.98; H, 7.05; N, 13.99. <sup>1</sup>H NMR: 1.45–1.47 (m, 4H, 2CH<sub>2</sub>), 1.76–1.78 (m, 4H, 2CH<sub>2</sub>), 2.61–2.63 (m, 8H, 4CH<sub>2</sub>), 2.76 (t, 4H, *J* = 6.2 Hz, 2CH<sub>2</sub>), 3.79–3.81 (m, 16H, 8CH<sub>2</sub>), 5.21 (s, 2H, 2NH), 7.36–7.45 (m, 4H, 4ArH), 7.70 (t, 2H, *J* = 7.5 Hz, 2ArH), 8.03–8.19 (m, 6H, 6ArH), 8.87 (d, 2H, *J* = 6.8 Hz, 2ArH), 12.44 (s, 2H, 2CONH). MALDI-MS: 782.9 (M + 1). Its tetrahydrochloride salt was obtained as a yellow powder, mp 217–219 °C.

**C6-DMAE Dimer.** This was prepared as for the C6-DMAE dimer, from *N*-[2-(*N*-dimethylamino)ethyl]-9-chloroacridine-4-carboxamide and hexamethylenediamine, and then flash chromatographed on alumina (ethyl acetate then methanol/chloroform) and recrystallized from ethyl acetate/petroleum ether as a yellow solid (60% yield), mp 98–100 °C. Found: C,

67.58; H, 7.56; N, 14.80. C<sub>42</sub>H<sub>50</sub>N<sub>8</sub>O·2.5H<sub>2</sub>O requires: C, 67.81; H, 7.45; N, 15.06. <sup>1</sup>H NMR: 1.35–1.37 (m, 4H, 2CH<sub>2</sub>), 1.67–1.69 (m, 4H, 2CH<sub>2</sub>), 2.39 (s, 12H, 2N(CH<sub>3</sub>)<sub>2</sub>), 2.67 (t, 4H, *J* = 6.2 Hz, 2CH<sub>2</sub>), 3.70–3.73 (m, 8H, 4CH<sub>2</sub>), 5.38 (br s, 2H, 2NH), 7.27–7.32 (m, 4H, 4ArH), 7.63 (t, 2H, *J* = 7.5 Hz, 2ArH), 7.97–8.02 (m, 4H, 4ArH), 8.12 (d, 2H, *J* = 8.2 Hz, 2ArH), 8.78 (br s, 2H, 2ArH), 12.52 (br s, 2H, 2CONH). MALDI-MS: 699.0 (M + 1). Its tetrahydrochloride salt was obtained as a yellow solid, mp 210–212 °C.

**C3NC3-morpholino Dimer.** This was prepared as for the C8-morpholino dimer, from *N*-[2-(*N*-morpholino)ethyl]-9-chloroacridine-4-carboxamide and *N*-(3-aminopropyl)-1,3-propanediamine, and then flash chromatographed on alumina (ethyl acetate/diisopropylamine, *v/v* = 10/1) and then methanol/diisopropylamine, *v/v* = 5/1) as an orange solid (52% yield), mp 127–129 °C. Found: C, 65.23; H, 6.88; N, 14.9. C<sub>46</sub>H<sub>55</sub>N<sub>9</sub>O<sub>4</sub>·2.5H<sub>2</sub>O requires: C, 65.53; H, 7.17; N, 14.99. <sup>1</sup>H NMR: 1.93–1.96 (m, 4H, 2CH<sub>2</sub>), 2.60–2.63 (m, 8H, 4CH<sub>2</sub>), 2.73–2.77 (m, 4H, 2CH<sub>2</sub>), 2.87–2.90 (m, 4H, 2CH<sub>2</sub>), 3.78–3.81 (m, 12H, 6CH<sub>2</sub>), 7.23–7.25 (m, 4H, 4ArH), 7.61 (m, 2H, 2ArH), 8.06–8.21 (m, 6H, 6ArH), 8.79 (m, 2H, 2 ArH), 12.52 (br s, 2H, 2CONH). MALDI-MS: 797.9 (M + 1). Its pentahydrochloride salt was obtained as a yellow solid, mp 226–229 °C.

**C3NC3-DMAE Dimer.** This was prepared as for the C3NC3-morpholino dimer, from *N*-[2-(*N*-dimethylamino)ethyl]-9-chloroacridine-4-carboxamide and *N*-(3-aminopropyl)-1,3-propane-diamine, and then flash chromatographed on alumina (ethyl acetate/diisopropylamine, *v/v* = 10/1) and then methanol/diisopropylamine, *v/v* = 5/1). The product obtained after column chromatography was still impure and was further treated with hot acetonitrile followed by cooling on ice. The dimer was now obtained as a sticky oil, which gradually solidified as a yellow solid (37% yield), mp 103–105 °C. <sup>1</sup>H NMR: 1.97–2.02 (m, 4H, 2CH<sub>2</sub>), 2.40 (s, 12H, 2N(CH<sub>3</sub>)<sub>2</sub>), 2.71 (t, 4H, *J* = 5.9 Hz, 2CH<sub>2</sub>), 2.87–2.91 (m, 4H, 2CH<sub>2</sub>), 3.70–3.74 (m, 4H, 2CH<sub>2</sub>), 3.92–3.97 (m, 4H, 2CH<sub>2</sub>), 5.42 (br s, 3H, 3NH), 7.16–7.21 (m, 4H, 4ArH), 7.56 (t, 2H, *J* = 7.4 Hz, 2ArH), 7.80 (d, 2H, *J* = 8.3 Hz, 2ArH), 8.09 (d, 2H, *J* = 8.3 Hz, 2ArH), 8.22 (d, 2H, *J* = 7.9 Hz, 2ArH), 8.53–8.56 (m, 2H, 2ArH), 11.80 (br s, 2H, 2CONH). MALDI-MS: 713.7 (M + 1). The microanalysis was carried out on its pentahydrochloride salt, a yellow solid, mp 246–249 °C. Found: C, 51.42; H, 6.86; N, 12.90. C<sub>42</sub>H<sub>51</sub>N<sub>9</sub>O<sub>2</sub>·5HCl·5H<sub>2</sub>O requires: C, 51.15; H, 6.74; N, 12.78.

**C4NC3-morpholino Dimer.** This was prepared as for the C8-morpholino dimer, from *N*-[2-(*N*-morpholino)ethyl]-9-chloroacridine-4-carboxamide and spermidine, and then purified by column chromatography (alumina, ethyl acetate then methanol/chloroform). The product was obtained as a yellow solid in 62% yield, mp 82–83 °C. <sup>1</sup>H NMR: 1.67–1.72 (m, 2H, CH<sub>2</sub>), 1.84 (t, 4H, *J* = 6.0 Hz, 2CH<sub>2</sub>), 2.59 (br s, 8H, 4CH<sub>2</sub>), 2.67–2.75 (m, 6H, 3CH<sub>2</sub>), 2.88 (*t-like*, 2H, CH<sub>2</sub>), 3.76–3.84 (m, 14H, 7CH<sub>2</sub>), 3.96 (*t-like*, 2H, CH<sub>2</sub>), 7.18 (t, 2H, *J* = 7.7 Hz, 2ArH), 7.26–7.31 (m, 2H, 2ArH), 7.55–7.65 (m, 2H, 2 ArH), 7.97–8.10 (m, 4H, 4 ArH), 8.17 (d, 2H, *J* = 8.1 Hz, 2 ArH), 8.70–8.78 (m, 2H, 2ArH), 12.48 (br s, 2H, 2CONH). MALDI-MS: 811.6 (M + 1). The microanalysis was carried out on its pentahydrochloride salt, a yellow solid, mp 232–234 °C. Found: C, 49.79; H, 6.58; N, 11.02. C<sub>47</sub>H<sub>57</sub>N<sub>9</sub>O<sub>4</sub>·5HCl·8H<sub>2</sub>O requires: C, 49.59; H, 6.90; N, 11.07.

**C4NC3-DMAE Dimer.** This was prepared as for the C4NC3-morpholino dimer, from *N*-[2-(*N*-dimethylamino)ethyl]-9-chloroacridine-4-carboxamide and spermidine. The product obtained after column chromatography (alumina, ethyl acetate then methanol/chloroform) was still not pure in this case, but it was found that the impurities could be extracted with warm ethyl acetate. The pure product was finally obtained as a yellow solid (in 41% yield) after recrystallization from ethyl acetate/methanol, mp 143–145 °C. Found: C, 67.97; H, 7.31; N, 16.28. C<sub>43</sub>H<sub>53</sub>N<sub>9</sub>O<sub>2</sub>·2H<sub>2</sub>O requires: C, 67.60; H, 7.52; N, 16.50. <sup>1</sup>H NMR: 1.69–1.74 (m, 2H, CH<sub>2</sub>), 1.82–1.89 (m, 4H, 2CH<sub>2</sub>), 2.40 (s, 12H, 2N(CH<sub>3</sub>)<sub>2</sub>), 2.67–2.72 (m, 6H, 3CH<sub>2</sub>), 2.91 (t, 2H, *J* = 5.8 Hz, CH<sub>2</sub>), 3.73–3.76 (m, 4H, 2CH<sub>2</sub>), 3.85 (t, 2H, *J* = 6.2 Hz, CH<sub>2</sub>), 4.01 (t, 2H, *J* = 5.8 Hz, CH<sub>2</sub>), 7.20–



7.36 (m, 4H, 4ArH), 7.57–7.66 (m, 2H, 2ArH), 7.92–8.23 (m, 6H, 6ArH), 8.70–8.76 (m, 2H, 2ArH), 12.43 (br s, 2H, 2CONH). MALDI-MS: 728.0 (M + 1). Its pentahydrochloride salt was obtained as a pale yellow solid, mp 239–242 °C.

**C6N2-morpholino Dimer.** This was prepared as for the C8-morpholino dimer, from *N*-[2-(*N*-morpholino)ethyl]-9-chloroacridine-4-carboxamide and anhydrous triethylenetetramine (obtained by azeotropic distillation with benzene for 16 h). The crude product obtained after normal workup was flash chromatographed on alumina gel (ethyl acetate and then methanol/chloroform) and then recrystallized from ethyl acetate as a yellow solid (in 34% yield), mp 152–154 °C. <sup>1</sup>H NMR: 2.61–2.66 (m, 12H, 6CH<sub>2</sub>), 2.77 (t, 4H, *J* = 6.1 Hz, 2CH<sub>2</sub>), 3.79–3.82 (m, 16H, 8CH<sub>2</sub>), 3.93–3.97 (m, 4H, 2CH<sub>2</sub>), 7.38–7.45 (m, 4H, 4ArH), 7.72 (t, 2H, *J* = 7.5 Hz, 2ArH), 8.13 (d, 2H, *J* = 8.6 Hz, 2ArH), 8.19 (d, 2H, *J* = 8.6 Hz, 2ArH), 8.31 (dd, 2H, *J* = 8.6, 1.1 Hz, 2ArH), 8.86 (d, 2H, *J* = 6.8 Hz, 2ArH), 12.49 (br s, 2H, 2CONH). MALDI-MS: 812.8 (M + 1). The microanalysis was carried out on its hexahydrochloride salt, a yellow solid, mp 220–222 °C. Found: C, 47.77; H, 6.90; N, 12.25. C<sub>46</sub>H<sub>56</sub>N<sub>10</sub>O<sub>4</sub>·6HCl·7H<sub>2</sub>O requires: C, 47.71; H, 6.62; N, 12.10.

**C6N2-DMAE Dimer.** This was prepared as for the C8-DMAE dimer, from *N*-[2-(*N*-dimethylamino)ethyl]-9-chloroacridine-4-carboxamide and triethylenetetramine. The product obtained after column chromatography on alumina (ethyl acetate then methanol/chloroform) was still impure; recrystallization from a variety of solvents was not successful. The clean free base was finally obtained by rebasification of its hydrochloride salt, which was purified by recrystallization from methanol/ethyl acetate, as a yellow solid (in 49% yield), mp 78–79 °C. <sup>1</sup>H NMR: 2.39 (s, 12H, 2N(CH<sub>3</sub>)<sub>2</sub>), 2.67 (*t-like*, 4H, 2CH<sub>2</sub>), 2.80–2.83 (m, 4H, 2CH<sub>2</sub>), 2.93–2.96 (m, 4H, 2CH<sub>2</sub>), 3.75 (*t-like*, 4H, 2CH<sub>2</sub>), 3.83–3.86 (m, 4H, 2CH<sub>2</sub>), 4.78 (br s, 3H, 3NH), 7.28–7.33 (m, 4H, 4ArH), 7.64 (t, 2H, *J* = 7.5 Hz, 2ArH), 7.99 (d, 2H, *J* = 7.5 Hz, 2ArH), 8.08 (d, 2H, *J* = 7.9 Hz, 2ArH), 8.21 (d, 2H, *J* = 7.9 Hz, 2ArH), 8.80–8.83 (m, 2H, 2ArH), 12.55 (br s, 2H, 2CONH). MALDI-MS: 729.1 (M + 1). The microanalysis was carried out on its hexahydrochloride salt, a yellow solid, mp 290 °C (dec). Found: C, 48.02; H, 6.86; N, 13.40. C<sub>42</sub>H<sub>52</sub>N<sub>10</sub>O<sub>2</sub>·6HCl·6H<sub>2</sub>O requires: C, 47.78; H, 6.68; N, 13.26.

**Preparation of 1,4-Bis(2-aminoethyl)piperazine.** Anhydrous sodium carbonate (10.6 g, 0.10 mol) was added, in a single portion, to a solution of piperazine (2.15 g, 25 mmol) and chloroacetonitrile (4.53 g, 60 mmol) in absolute ethanol (100 mL). The whole was then refluxed with stirring for 4 h. The hot mixture was filtered and the insoluble part washed with hot ethanol and filtered again. The combined filtrate was condensed to about 40 mL and then cooled on ice. 1,4-Bis-(ethanenitrile)piperazine crystallized from the solution as white needles (3.47 g, 85%), mp 165–166 °C (lit.<sup>42</sup> mp 165 °C). <sup>1</sup>H NMR: 2.66 (s, 8H, 4CH<sub>2</sub>), 3.52 (s, 4H, 2CH<sub>2</sub>). To a mixture of the above bis(ethane)nitrile compound (1.64 g, 10 mmol) in *N*-ethylmorpholine (25 mL), was added, in portions, lithium aluminum hydride (0.91 g, 24 mmol) over 30 min under a nitrogen atmosphere. The resulting mixture was refluxed with stirring for 1 h under nitrogen and then cooled to room temperature. The insoluble material was filtered off, diethyl ether (80 mL) was added to the filtrate, and the whole was stored at 4 °C overnight. The oil which appeared was decanted, washed repeatedly with diethyl ether, and dried in a vacuum desiccator. 1,4-Bis(2-aminoethyl)piperazine was then obtained as a viscous oil and was used in the following steps without further purification. <sup>1</sup>H NMR: 2.36–2.46 (m, 12H, 4CH<sub>2</sub>+2NH<sub>2</sub>), 2.77 (t, 4H, *J* = 6.2 Hz, 2CH<sub>2</sub>).

**C2pipC2-morpholino Dimer.** This was prepared as for the C8-morpholino dimer, from *N*-[2-(*N*-morpholino)ethyl]-9-chloroacridine-4-carboxamide and 1,4-bis(2-aminoethyl)piperazine. The product obtained after column chromatography on alumina (ethyl acetate and then methanol/chloroform) was still not pure and was recrystallized from ethyl acetate/methanol to afford the pure dimer as a pale yellow solid (31% yield), mp 200–201 °C. Found: C, 65.97; H, 6.84; N, 16.15.

C<sub>48</sub>H<sub>58</sub>N<sub>10</sub>O<sub>4</sub>·2H<sub>2</sub>O requires: C, 65.88; H, 7.14; N, 16.01. <sup>1</sup>H NMR: 2.62–2.80 (m, 24H, 12CH<sub>2</sub>), 3.80–3.83 (m, 12H, 6CH<sub>2</sub>), 3.93–3.97 (m, 4H, 2CH<sub>2</sub>), 6.69 (br s, 2H, 2NH), 7.38–7.48 (m, 4H, 4ArH), 7.72 (t, 2H, *J* = 7.5 Hz, 2ArH), 8.13–8.21 (m, 4H, 4ArH), 8.31 (d, 2H, *J* = 8.4 Hz, 2ArH), 8.87 (d, 2H, *J* = 7.1 Hz, 2ArH), 12.48 (br s, 2H, 2CONH). MALDI-MS: 839.3 (M + 1). Its hexahydrochloride salt was obtained as a yellow solid, mp 271 °C (dec).

**C2pipC2-DMAE Dimer.** This was prepared as for the C8-DMAE dimer, from *N*-[2-(*N*-dimethylamino)ethyl]-9-chloroacridine-4-carboxamide and 1,4-bis(2-aminoethyl)piperazine, and purified by column chromatography (alumina, ethyl acetate/diisopropylamine (v:v = 50:1) and then methanol/chloroform). The free base was obtained as a yellow solid (in 48% yield), which become dark on standing in the air. <sup>1</sup>H NMR: 2.42 (s, 12H, 2N(CH<sub>3</sub>)<sub>2</sub>), 2.68–2.76 (m, 16H, 8CH<sub>2</sub>), 3.77 (q, 4H, *J* = 5.7 Hz, 2CH<sub>2</sub>), 3.92 (t, 4H, *J* = 5.7 Hz, 2CH<sub>2</sub>), 6.68 (br s, 2H, 2NH), 7.38–7.45 (m, 4H, 4ArH), 7.70 (t, 2H, *J* = 7.4 Hz, 2ArH), 8.05 (d, 2H, *J* = 8.6 Hz, 2ArH), 8.16 (d, 2H, *J* = 8.6 Hz, 2ArH), 8.28 (dd, 2H, *J* = 8.5 Hz, 1.1 Hz, 2ArH), 8.85 (d, 2H, *J* = 6.8 Hz, 2ArH), 12.53 (br s, 2H, 2CONH). MALDI-MS: 755.5 (M + 1). The microanalysis was carried out on its hexahydrochloride salt, a yellow solid, mp 217–218 °C. Found: C, 49.52; H, 6.45; N, 13.45. C<sub>44</sub>H<sub>54</sub>N<sub>10</sub>O<sub>2</sub>·6HCl·5H<sub>2</sub>O requires: C, 49.68; H, 6.63; N, 13.17.

**DNA Helix Unwinding Assay.** Covalently closed circular plasmid DNA, pBR 322, isolated from *E. coli* (*dam*<sup>+</sup>, *dcm*<sup>+</sup>), was purchased from Progen Industries Ltd as a 0.5 mg per mL solution in 10 mM Tris-HCl buffer, pH 7.5. It was found to be 90% in the supercoiled form by measurement of the relative intensities of ethidium-stained bands for the closed circular and nicked circular forms on agarose gels. Ethidium bromide was purchased from Amresco Ltd. and used without further purification. The agarose used was DNA grade as supplied by Progen Industries Ltd. Ultrapure grade Tris base [tris(hydroxymethyl)aminomethane] was purchased from Amresco Ltd and analytical grade glacial acetic was from Scharlau Ltd. Drug solutions were prepared in 40 mM TAE buffer (40 mM tris(hydroxymethyl)aminomethane, 30 mM glacial acetic acid, 1 mM EDTA, pH 7.5) at the required concentrations; hence 5 μL of solution was mixed with an equal volume of a 30 μg per mL solution of pBR 322 DNA (150 ng of DNA, 23.6 μM in base pairs) in TAE buffer pH 7.5. Complexes were incubated in the dark for 1 h at room temperature prior to application to the agarose gel. Each titration was repeated at least three times, and the precision in the value of the unwinding angles was determined by the width of the equivalence points. To prepare the gel, 1.2 g of agarose was dissolved in 150 mL of TAE buffer, giving a concentration of 0.8% by heating to about 55 °C. The solution was cooled to 30 °C and poured onto a gel plate to set, and the plate was placed in an electrophoresis apparatus and submerged in TAE buffer to a depth of 1 mm. Following incubation of the DNA and drug, 3 μL of loading buffer [0.25% (w/v) bromophenol blue and 30% (w/v) glycerol] was mixed with the complex samples, and the samples were loaded onto the gel. Electrophoresis was continued for 1 h and 15 min at 74 V (5 V/cm) at room temperature. After electrophoresis, the gel was stained for 30 min by placing it in a TAE bath (250 mL) containing 1 μg per mL of ethidium bromide, and the fluorescence emission contrast was enhanced by destaining in a TAE bath for an additional 20 min. The gel was transilluminated by UV light and fluorescence emission visualized by a CCD camera coupled to a Bio-Rad Gel Doc 2000 apparatus. Bio-Rad Multianalyst 1.20 software was used to capture the image as TIFF files, which were later manipulated with PhotoShop Adobe 6.0 for graphical presentation. On occasions, helix-unwinding experiments were performed in buffer containing 40 mM BisTris (2-[bis(2-hydroxyethyl)amino]-2-(hydroxymethyl)propane-1,3-diol-(hydroxymethyl) methane), 30 mM glacial acetic acid, 1 mM EDTA, pH 6.1.

**DNA Dissociation Kinetics.** Actinomycin D and calf thymus DNA, sodium salt type I, were purchased from Sigma-Aldrich, and used without further purification. A stock solution



of 1 M SHE buffer containing 0.2 M 4-(2-hydroxyethyl)-1-piperazine-ethanesulfonic acid, 10 mM EDTA, and 1 M sodium chloride was adjusted to pH 7.0 using NaOH. A 100-fold dilution of this buffer, 0.01 SHE, was used for dissolving and dialysing DNA. The experimental buffer used for spectrophotometric and kinetic measurements, designated 0.1 SHE, was prepared by adding sufficient solid NaCl to 0.01 SHE buffer to bring the NaCl concentration to 0.1 M. The calf thymus DNA was sonicated to reduce its viscosity, so as to facilitate efficient mixing with SDS solutions. Kinetic measurements were performed using a Cary 50 spectrophotometer utilizing the Cary Win UV Kinetics software (Varian Inc.). A 900  $\mu$ L portion of a DNA–ligand complex solution comprising 555  $\mu$ M DNA and 55  $\mu$ M ligand in 0.1 SHE buffer was mixed with 100  $\mu$ L of 200 mM SDS solution in 0.1 SHE buffer in a 1 mL semi-microquartz cuvette at 23 °C. Thus the final concentrations were 500  $\mu$ M in DNA, 50  $\mu$ M in ligand, and 20 mM in SDS. The ligand-to-DNA ratio before dissociation was 0.1, so that there was one drug molecule bound per turn of the duplex. To ensure rapid mixing, the solutions were simultaneously injected into the cuvette using Gilson pipets. The DNA–ligand complex had been previously equilibrated at room temperature for 1 h. Data were collected at the wavelength where the difference between the absorbance of the DNA-bound ligand and the ligand in SDS micelles was greatest, which for the bis(9-aminoacridine-4-carboxamides) was 423 nm and for actinomycin D was 430 nm. A total of 2000 data points were collected for each kinetic run at three different sampling frequencies, distributed proportionately according to the magnitude of the changing absorbance signal. The final equilibrium absorbance was also experimentally determined. Total sweep times were in the range 420–3600 s. The primary absorbance data were manipulated to express measured absorbances as a fraction of the total equilibrium absorbance change, so as to cast them as a dimensionless fraction of reaction. Such progress curves were then analyzed for multiple exponential components by using a nonlinear least squares facility in the Origin v 7.0 software package (OriginLab). The curves were deconvoluted into one to three exponentials using the Levenberg–Marquardt algorithm employing analytical partial differentials to find the curve of best fit, as determined by minimizing Gaussian standard errors of the residuals. Residual plots were generated to enable a visual inspection of the goodness of fit. Final data are the average of five separate kinetic runs.

**Cell Line.** CCRF-CEM, a human lymphoblastoid (T-cell leukemia) cell line<sup>32</sup> was obtained from Dr. Maria Kavallaris, Childrens Cancer Research Institute, Sydney, Australia, and maintained in RPMI medium 1640 (Gibco BRL) supplemented with 2 mM l-glutamine, 100 units/mL of penicillin/streptomycin, and 10% foetal bovine serum (Trace) at 37 °C, in the presence of 5% CO<sub>2</sub>.

**Growth Inhibition Assay.** Cells were seeded at a density of  $1 \times 10^5$  cells/mL and adjusted to a final volume of 1.6 mL with RPMI medium in 24-well plates. The test agent, dissolved at 1 mM concentration in deionized water, was diluted in phosphate-buffered saline to 400  $\mu$ L at a range of concentrations before addition to the cell suspension. Drug-treated cells were incubated for at least four rounds of division and counted on a Coulter Counter after 72 h. Each drug concentration was measured in duplicate, the whole growth inhibition curve being repeated at least three times. Control cells were treated in a similar way, save they received the addition of 400  $\mu$ L of medium instead of drug. The concentration of drug required to inhibit growth by 50% compared to the control, the IC<sub>50</sub> value, was obtained using a sigmoidal plotting function provided in the GraphPad Prism software.

**Flow Cytometry.** Cells were seeded at a density of  $1 \times 10^5$  cells/mL in 25 mL flasks, and incubated for 24 h before addition of drugs. Drug samples dissolved in phosphate-buffered saline were then added at 1, 2, 5, and 10 times the measured IC<sub>50</sub> concentrations, and the cells were incubated for a further 24 and 48 h. Suitable control cells, without the addition of drugs, were prepared in a similar manner. The cells

were then washed in phosphate-buffered saline and fixed in ice-cold ethanol for at least 2 h before analysis, where after they were stained with propidium iodide as outlined in *Current Protocols in Cytometry 2*, and analyzed on a Becton-Dickson FACSort, using CellQuest software. These measurements provided cell cycle profiles as determined by assessing total DNA content and were used to evaluate the proportion of cells in the various stages of the cycle in the presence of the drugs after 24 and 48 h of exposure.

**Abbreviations.** DACA, N-[2-(dimethylamino)ethyl]acridine-4-carboxamide; 9-amino-DACA, 9-amino-N-(2-(dimethylamino)ethyl)acridine-4-carboxamide; DMAE, N,N-dimethylaminoethyl; SDS, sodium dodecyl sulfate.

**Acknowledgment.** This work was supported by the Australian National Health and Medical Research Council (L.P.G.W., B.W.S.).

**Supporting Information Available:** Flow cytometric profiles. This material is available free of charge via the Internet at <http://pubs.acs.org>.

## References

- (1) Liu, L. F. DNA topoisomerase poisons as antitumor drugs. *Annu. Rev. Biochem.* **1989**, *58*, 351–75.
- (2) Malonne, H.; Atassi, G. DNA topoisomerase targeting drugs: Mechanisms of action and perspectives. *Anticancer Drugs* **1997**, *8*, 811–22.
- (3) Kellner, U.; Sehested, M.; Jensen, P. B.; Gieseler, F.; Rudolph, P. Culprit and victim -- DNA topoisomerase II. *Lancet Oncol.* **2002**, *3*, 235–43.
- (4) Verweij, J.; den Hartigh, J.; Pinedo, H. M. Antitumor antibiotics. In *Cancer Chemotherapy: Principles and Practice*; Chabner, B. A., Collins, J. M., Eds.; J. B. Lippincott Co.: Philadelphia, 1990; pp 382–96.
- (5) Denny, W. A.; Roos, I. A. G.; Wakelin, L. P. G. Interrelations between antitumour activity, DNA breakage, and DNA binding kinetics for 9-aminoacridinecarboxamide antitumor agents. *Anti-Cancer Drug Des.* **1986**, *1*, 141–7.
- (6) Bridewell, D. J.; Finlay, G. J.; Baguley, B. C. Topoisomerase I/II selectivity among derivatives of N-[2-(dimethylamino)ethyl]acridine-4-carboxamide (DACA). *Anti-Cancer Drug Des.* **2001**, *16*, 317–24.
- (7) Caponigro, F.; Dittrich, C.; Sorensen, J. B.; Schellens, J. H.; Duffaud, F.; Paz Ares, L.; Lacombe, D.; de Balincourt, C.; Fumoleau, P. Phase II study of XR 5000, an inhibitor of topoisomerases I and II, in advanced colorectal cancer. *Eur. J. Cancer* **2002**, *38*, 70–4.
- (8) Muller, W.; Crothers, D. M. Studies of the binding of actinomycin and related compounds to DNA. *J. Mol. Biol.* **1968**, *35*, 251–90.
- (9) Waring, M. J.; Wakelin, L. P. G. Echinomycin: A bifunctional intercalating antibiotic. *Nature* **1974**, *25*, 653–657.
- (10) Searle, M. S.; Hall, J. G.; Denny, W. A.; Wakelin, L. P. G. NMR studies of the interaction of the antibiotic nogalamycin with the hexadeoxyribonucleotide duplex d(5'-GCATGC)2. *Biochemistry* **1988**, *27*, 4340–4349.
- (11) Farber, S.; D'Angio, G.; Evans, A.; Mitus, A. Clinical studies of actinomycin D with special reference to Wilms' tumor in children. *J. Urol.* **2002**, *168*, 2560–2.
- (12) Gradishar, W. J.; Vogelzang, N. J.; Kilton, L. J.; Leibach, S. J.; Rademaker, A. W.; French, S.; Benson, A. B., III. A phase II clinical trial of echinomycin in metastatic soft tissue sarcoma. An Illinois Cancer Center Study. *Invest. New Drugs* **1995**, *13*, 171–4.
- (13) Kamitori, S.; Takusagawa, F. Crystal structure of the 2:1 complex between d(GAAGCTTC)<sub>2</sub> and the anticancer drug actinomycin D. *J. Mol. Biol.* **1992**, *225*, 445–56.
- (14) Ughetto, G.; Wang, A. H.; Quigley, G. J.; van der Marel, G. A.; van Boom, J. H.; Rich, A. A. Comparison of the structure of echinomycin and triostin A complexed to a DNA fragment. *Nucleic Acids Res.* **1985**, *13*, 2305–23.
- (15) Fox, K. R.; Brassett, C.; Waring, M. J. Kinetics of dissociation of nogalamycin from DNA: Comparison with other anthracycline antibiotics. *Biochim. Biophys. Acta* **1985**, *840*, 383–92.
- (16) Fox, K. R.; Wakelin, L. P. G.; Waring, M. J. Kinetics of the interaction between echinomycin and DNA. *Biochemistry* **1981**, *20*, 5768–5779.
- (17) Wakelin, L. P. G.; Atwell, G. J.; Rewcastle, G. W.; Denny, W. A. Relationships between DNA binding kinetics and biological activity for the 9-aminoacridine-4-carboxamide class of antitumour agent. *J. Med. Chem.* **1987**, *30*, 855–861.
- (18) Denny, W. A.; Wakelin, L. P. G. Kinetics of the binding of mitoxantrone, ametantrone and analogues to DNA: Relationship to binding mode and antitumour activity. *Anti-Cancer Drug Des.* **1990**, *5*, 189–200.

- (19) Wakelin, L. P. G.; Adams, A.; Denny, W. A. Kinetic studies of the binding of acridinecarboxamide topoisomerase poisons to DNA: Implications for the mode of binding of ligands with uncharged chromophores. *J. Med. Chem.* **2002**, *45*, 894–901.
- (20) Wakelin, L. P. G.; Chetcuti, P.; Denny, W. A. Kinetic and equilibrium studies of amsacrine-4-carboxamides: A class of asymmetrical DNA intercalating agent which must bind by threading through the DNA helix. *J. Med. Chem.* **1990**, *33*, 2039–2044.
- (21) Adams, A.; Collyer, C.; Guss, M.; Denny, W. A.; Wakelin, L. P. G. Crystal structure of the topoisomerase II poison 9-amino-[N-(2-dimethylamino)ethyl]acridine-4-carboxamide bound to the DNA hexanucleotide d(CGTACG)<sub>2</sub>. *Biochemistry* **1999**, *38*, 9221–9233.
- (22) Adams, A.; Guss, J. M.; Denny, W. A.; Wakelin, L. P. G. Crystal Structure of 9-amino[N-(2-morpholino)ethyl]acridine-4-carboxamide bound to d(CGTACG)<sub>2</sub>: Implications for Structure Activity Relationships of Acridinecarboxamide Topoisomerase Poisons. *Nucleic Acids Res.* **2002**, *30*, 719–725.
- (23) Denny, W. A. DNA-intercalating ligands as anti-cancer drugs: Prospects for future design. *Anti-Cancer Drug Des.* **1989**, *4*, 241–263.
- (24) Leng, F.; Priebe, W.; Chaires, J. B. Ultratight DNA binding of a new bisintercalating anthracycline antibiotic. *Biochemistry* **1998**, *37*, 1743–53.
- (25) Murr, M. M.; Harting, M. T.; Guelev, V.; Ren, J.; Chaires, J. B.; Iverson, B. L. An octakis-intercalating molecule. *Bioorg. Med. Chem.* **2001**, *9*, 1141–8.
- (26) Miller, C. T.; Weragoda, R.; Izbicka, E.; Iverson, B. L. The synthesis and screening of 1,4,5,8-naphthalenetetracarboxylic diimide-peptide conjugates with antibacterial activity. *Bioorg. Med. Chem.* **2001**, *9*, 2015–24.
- (27) Wakelin, L. P. G. Polyfunctional DNA intercalating agents. *Med. Res. Rev.* **1986**, *6*, 275–340.
- (28) Chow, K.-C.; Ross, W. E. Topoisomerase-specific drug sensitivity in relation in cell cycle progression. *Mol. Cell. Biol.* **1987**, *7*, 3119–23.
- (29) Sleiman, R. J.; Catchpole, D. R.; Stewart, B. W. Drug-induced death of leukaemic cells after G2/M arrest: Higher order DNA fragmentation as an indicator of mechanism. *Br. J. Cancer* **1998**, *77*, 40–50.
- (30) Kohn, K. W.; Jackman, J.; O'Connor, P. M. Cell cycle control and cancer chemotherapy. *J. Cell Biol.* **1994**, *54*, 440–52.
- (31) Hannun, Y. A. Apoptosis and the dilemma of cancer chemotherapy. *Blood* **1997**, *89*, 1845–53.
- (32) Sleiman, R. J.; Stewart, B. W. Early caspase activation in leukemic cells subject to etoposide-induced G2-M arrest: Evidence of commitment to apoptosis rather than mitotic cell death. *Clin. Cancer Res.* **2000**, *6*, 3756–65.
- (33) Del Bino, G.; Skierski, J. S.; Darzynkiewicz, Z. Diverse effects of camptothecin, an inhibitor of topoisomerase I, on the cell cycle of lymphocytic (L1210, MOLT-4) and myelogenous (HL-60, KG1) leukemic cells. *Cancer Res.* **1990**, *50*, 5746–50.
- (34) Rene, B.; Fosse, P.; Khelifa, T.; Jacquemin-Sablon, A.; Bailly, C. Cytotoxicity and interaction of amsacrine derivatives with topoisomerase II: Role of the 1' substitute on the aniline nucleus. *Bull. Cancer* **1997**, *84*, 941–8.
- (35) Arlin, Z. A. Mitoxantrone and amsacrine: Two important agents for the treatment of acute myelogenous leukemia (AML) and acute lymphoblastic leukemia (ALL). *Bone Marrow Transplant* **1989**, *4 Suppl 1*, 57–9.
- (36) Rewcastle, G. W.; Denny, W. A. The synthesis of substituted 9-oxoacridan-4-carboxylic acids; Part 2. The use of 2-Iodoisophthalic acid in the Jourdan-Ullmann Reaction. *Synthesis* **1985**, 217–220.
- (37) Adams, A.; Guss, J. M.; Collyer, C. A.; Denny, W. A.; Prakash, A. S.; Wakelin, L. P. G. Acridinecarboxamide topoisomerase poisons: Structural and kinetic studies of the DNA complexes of 5-substituted 9-amino-(N-(2-dimethylamino)ethyl)-acridine-4-carboxamides. *Mol. Pharmacol.* **2000**, *58*, 649–658.
- (38) D'Rozario, A. P.; Greig, D. J.; Hudson, R. F.; Williams, A.; Stepwise Proton Transfer in the Acid-catalysed Hydrolysis of 3,1-Benzoxazin-4-ones: Electrostatic or Hydrogen-bond Stabilisation of the Conjugate Acid. *J. Chem. Soc., Perkin Trans. 2* **1981**, 590–596.
- (39) Sumpter, W. C.; Jones, W. F. The Nitration of Isatin. *J. Am. Chem. Soc.* **1943**, *65*, 1802–1803.
- (40) Deady, L. W.; Kaye, A. J.; Finlay, G. J.; Baguley, B. C.; Denny, W. A. Synthesis and antitumor properties of N-[2-(dimethylamino)ethyl]carboxamide derivatives of fused tetracyclic quinolines and quinoxalines: A new class of putative topoisomerase inhibitors. *J. Med. Chem.* **1997**, *40*, 2040–6.
- (41) Atwell, G. J.; Cain, B. F.; Baguley, B. C.; Finlay, G. J.; Denny, W. A. Potential antitumor agents. 43. Synthesis and biological activity of dibasic 9-aminoacridine-4-carboxamides, a new class of antitumor agent. *J. Med. Chem.* **1984**, *27*, 1481–85.
- (42) Adelson, D. E.; Polland, C. B. Derivatives of Piperazine. IV. Reactions with Derivatives of Monochloroacetic Acid. *J. Am. Chem. Soc.* **1935**, *57*, 1280–81.
- (43) Chiari, B.; Piovesana, O.; Tarantelli, T.; Zanazzi, P. F. Exchange interaction in multinuclear transition-metal complexes. 5. Through-bond exchange coupling in Cu<sub>2</sub>A(CH<sub>3</sub>COO)<sub>2</sub>.2CH<sub>3</sub>OH (A<sup>2-</sup> = anion of N,N-bis(2-(6-hydroxybenzhydrylidene)-amino)-ethyl)piperazine). *Inorg. Chem.* **1984**, *23*, 2542–47.
- (44) Denny, W. A.; Atwell, G. J.; Baguley, B. C.; Wakelin, L. P. G. Potential antitumor agents. Part 44. Synthesis and antitumor activity of new classes of diacridines: The importance of linker chain rigidity for DNA-binding kinetics and antitumor activity. *J. Med. Chem.* **1985**, *28*, 1568–81.
- (45) Nielsen, P. E.; Zhen, W. P.; Henriksen, U.; Buchardt, O. Sequence-influenced interactions of oligoacridines with DNA detected by retarded gel electrophoretic migrations. *Biochemistry* **1988**, *27*, 67–73.
- (46) Chen, S. F.; Bhenrens, D. L.; Czerniak, P. M.; Dexter, D. L.; Dusak, B. J.; Fredericks, J. R.; Gale, K. C.; Gross, J. L.; Krishenbaum, M. R.; McRipley, L. M.; Patten, A. D.; Perella, F. W.; Seltz, S. P.; Stafford, M. P.; Sun, J. H.; Sun, T.; Wuonola, M. A.; von Hoff, D. D. XB596, a promising bis-naphthalimide anti-cancer agent. *Anticancer Drugs* **1993**, *4*, 447–457.
- (47) Fritzsche, H.; Triebel, H.; Chaires, J. B.; Dattagupta, N.; Crothers, D. M. Studies on the interaction of anthracycline antibiotics and deoxyribonucleic acid: Geometry of intercalation of iremycin and daunomycin. *Biochemistry* **1982**, *21*, 3940–3946.
- (48) Bauer, W. R. Structure and reactions of closed duplex DNA. *Annu. Rev. Biophys. Bioeng.* **1978**, *7*, 287–313.
- (49) Gao, X. L.; Mirau, P.; Patel, D. J. Structure refinement of the chromomycin dimer-DNA oligomer complex in solution. *J. Mol. Biol.* **1992**, *223*, 259–79.
- (50) Blagosklonny, M. V.; Pardee, A. B. Exploiting cancer cell cycling for selective protection of normal cells. *Cancer Res.* **2001**, *61*, 4301–5.
- (51) Solary, E.; Droin, N.; Sordet, O.; Rebe, C.; Filomenko, R.; Wotawa, A.; Plenchette, S.; Ducoroy, P. Cell death pathways as targets for anticancer drugs. In *Anticancer Drug Development*; Baguley, B. C., Kerr, D. J., Eds.; Academic Press: San Diego, 2002; pp 55–76.
- (52) Waldmann, H. Isatin-carboxylic acid. *J. Prakt. Chem.* **1937**, *147*, 338–43.
- (53) Lown, J. W.; Morgan, A. R.; Yen, S. F.; Wang, Y. H.; Wilson, W. D. Characteristics of the binding of the anticancer agents mitoxantrone and ametantrone and related structures to deoxyribonucleic acids. *Biochemistry* **1985**, *24*, 4028–35.
- (54) Waring, M. J. DNA-binding characteristics of acridinylmethane-sulphonamide drugs: Comparison with antitumor properties. *Eur. J. Cancer* **1976**, *12*, 995–1001.
- (55) Waring, M. J. Variation of the supercoils in closed circular DNA by binding of antibiotics and drugs: Evidence for molecular models involving intercalation. *J. Mol. Biol.* **1970**, *54*, 247–279.

JM030253D